TAMPEREEN TEKNILLINEN YLIOPISTO
TAMPERE UNIVERSITY OF TECHNOLOGY

Maija Hoikkanen

Injection Moulded Thermoplastic Elastomer – Metal Hybrids

Julkaisu 1024 • Publication 1024

Tampere 2012

Tampereen teknillinen yliopisto. Julkaisu 1024
Tampere University of Technology. Publication 1024

Maija Hoikkanen

Injection Moulded Thermoplastic Elastomer – Metal Hybrids

Thesis for the degree of Doctor of Science in Technology to be presented with due permission for public examination and criticism in Konetalo Building, Auditorium K1702, at Tampere University of Technology, on the 9th of March 2012, at 12 noon.

Tampereen teknillinen yliopisto - Tampere University of Technology
Tampere 2012

ISBN 978-952-15-2777-7 (printed)
ISBN 978-952-15-2793-7 (PDF)
ISSN 1459-2045

ABSTRACT

Thermoplastic – metal hybrids are a recent addition to material space. They are macroscopic composites of thermoplastic and metal with a defined structure formed during manufacturing and possess properties from both material groups. This study examines manufacturing, properties and structure of new kind of insert injection moulded thermoplastic elastomer (TPE) – metal hybrids. The bonding of TPE to planar metal surfaces was reached either through micromechanical anchoring or via use of a chemical coupling agent. The first approach was studied with poly(styrene-*block*-ethylene-*co*-butylene-*block*-styrene) (SEBS) – aluminium hybrids; the latter one with thermoplastic urethane (TPU) – N-(β-aminoethyl)-γ-aminopropyltrimethoxysilane – aluminium/stainless steel/copper hybrids.

The main injection moulding parameters related to adhesive strength were first studied with micromechanically bonded hybrids. Increasing the ratio of cavity depth to insert thickness increased the bond strength until saturation was reached. The most important injection moulding machine setting for maximizing the bond strength was the mould temperature. Both these effects are based on the polymer melt penetration into the microcavities at the metal surface. Compared to micromechanical bonding, the best hybrids bonded with chemical coupling agent had an order of magnitude higher bond strength. The focus with hybrids bonded with chemical coupling agent was set on comparisons between different metals and their surface modifications combined with the effects of silanization parameters on silane layer formation and bonding to TPU.

The silane layers on as-received stainless steel or copper were uneven. Similar behaviour was also observed for silane on electrolytically polished substrates with thin Fe/Cr mixed oxide layer. A homogenous, thick silane layer was formed after oxidation treatment independent on the oxide structure, and on stainless steel the thickness of the silane layer was dependent on the silane concentration. The coating evenness and thickness were linked to the bond strength in corresponding TPU – metal hybrids for both copper and stainless steel; the bond strength was more sensitive to the surface modification in the case of copper. With thick silane layers the failure was mainly cohesive in the silane layer and with optimal thin layers cohesive in TPU. Contrary to stainless steel and copper, in case of aluminium an interpenetrating oxide /siloxane layer is suggested to form.

Also the long-term environmental resistance of hybrids of TPU and selected metal substrates was studied. High humidity exposure led to depolymerization of the polysiloxane and deterioration of the bond in all occassions. After high temperature exposure the bond strength increased, except for hybrids of oxidized stainless steel. Based on the analysis of the exposed samples, it was deduced that the bond mechanism at the metal/silane interface is dependent on the metal oxide and its isoelectric point, except for aluminium, where Al oxide continues to grow during silanization.

PREFACE

This work was carried out at Department of Materials Science, Tampere University of Technology, Finland, during the years of 2005-2011. The work was partly conducted in the frame of two Finnish Funding Agency for Technology and Innovation (TEKES) projects, Hybrid products and In-Mold Integrated Structures (2005-2008), and Light and Wear Resistant Hybrid Materials (2009-2011). I also gratefully acknowledge the important support from Graduate School of Processing of Polymers and Polymer-Based Multimaterials.

I sincerely thank my supervisor Prof. Jyrki Vuorinen for long discussions and guidance on my topic, as well as on general material science and engineering. Thank you also for continuous encouragement and enthusiasm towards my work. My special thanks go to all of my co-authors. I have collaborated closely with Mr. Petri Fabrin and Dr. Mari Honkanen – thank you, we have come a long way together. I am also grateful to all three of them, as well as to Prof. Toivo Lepistö and Dr. Minnamari Vippola for fruitful discussions we shared with the whole research team. Also I especially thank Dr. Vippola for her detailed comments on my papers and this manuscript. I am also indebted to the laboratory staff for their help with the experimental work.

I thank all my past and present colleagues at Department of Materials Science. I have learned something and got help from all of you. Especially Ms. Tiina Hallila and Mr. Tommi Berg are thanked for daily discussions. And last but not least, I thank my family and friends for their support and encouragement.

LIST OF ORIGINAL PUBLICATIONS

This thesis is based on the following Publications I to VI.

I. P. Fabrin, M. Hoikkanen, J. Vuorinen, Adhesion of Thermoplastic Elastomer on Surface Treated Aluminum by Injection molding, *Polymer Engineering & Sci*ence 47 (2007) 1187-1191.

II. P. Fabrin, M. Hoikkanen, J. Vuorinen, Injection Molding of Thermoplastic Elastomer on Etched Aluminum: Taguchi Optimization. *SPE ANTEC Technical Papers 2007*, p. 2514-2518.

III. M. Hoikkanen, M. Honkanen, M. Vippola, T. Lepistö, J. Vuorinen, Effect of silane treatment parameters on the silane layer formation and bonding to thermoplastic urethane. *Progress in Organic Coatings* 72 (2011) 716-723.

IV. M. Honkanen, M. Hoikkanen, M. Vippola, J. Vuorinen, T. Lepistö, P. Jussila, H. Ali-Löytty, M. Lampimäki, M. Valden, Characterization of Silane Layer in Stainless Steel-TPU Hybrids. *Applied Surface Science* 257 (2011) 9335-9346.

V. M. Honkanen, M. Hoikkanen, M. Vippola, J. Vuorinen, T. Lepistö, Aminofunctional Silane Layers for Improved Copper – Polymer Interface Adhesion. *Journal of Materials Science* 46 (2011) 6618–6626.

VI. M. Hoikkanen, M. Honkanen, L. Frisk, M. Vippola, T. Lepistö, J. Vuorinen, Metal-TPU Hybrids in Environmental Exposure. *International Journal of Adhesion and Adhesives* 35 (2012) 21-26.

AUTHOR´S CONTRIBUTION

Publication I:
Together with the first author, the author shared the experimental work, interpretation of the results and writing the paper.

Publication II:
Together with the first author, the author shared the experimental work, interpretation of the results and writing the paper.

Publication III:
The author wrote the paper and is the corresponding author. She performed most of the experimental work and interpreted the results. M. Honkanen performed all scanning electron microscopy and atomic force microscopy studies.

Publication IV:
The author participated in planning and performing the experimental work, and commenting the paper. M. Honkanen performed all microscopical studies. P. Jussila, H. Ali-Löytty, M. Lampimäki and M. Valden are responsible of the XPS work.

Publication V:
The author participated in planning and performing the experimental work, interpreting the results and writing the paper. M. Honkanen performed all scanning electron microscopy, transmission electron microscopy and atomic force microscopy studies.

Publication VI:
The author wrote the paper and is the corresponding author. She performed most of the experimental work and interpreted the results. M. Honkanen performed all scanning electron microscopy studies. L. Frisk contributed to environmental testing.

TABLE OF CONTENTS

NOMENCLATURE

γ-AEAPS	γ-aminoethylaminopropyltrimethoxysilane
AFM	Atomic force microscopy
aq.	Aqueous
AISI	American Iron and Steel Institute
ANOVA	Analysis of variance
γ-APS	γ-aminopropyltriethoxysilane
ASTM	American Society for Testing and Materials
ATR	Attenuated total reflection
BIW	Body-in white
Cu-DHP	Phosporous deoxidized copper
DOE	Design of experiments
DSC	Differential scanning calorimetry
E	Young´s modulus
f	Fibre volume fraction
FESEM	Field emission scanning electron microscopy
FT-IR	Fourier transform infrared spectroscopy
γ-GPS	γ-glycidoxypropyltrimethoxysilane
IEP	Isoelectric point
IPN	Interpenetrating network
MDI	Methylene-4,4´-diphenyl di-isocyanate
MSD	Mean squared deviation
OFE-OK	Oxygen-free, high conductivity copper
OM	Optical microscopy
PBT	Polybutyleneterephthalate
PC	Polycarbonate
PP	Polypropene
PPS	Polyphenylenesulphide
PVC	Polyvinylchloride
R_a	Arithmetic mean of surface roughness
RAIRS	Reflection-absorption infrared spectroscopy
RH	Relative humidity, %
SEBS	Poly(styrene-*block*-ethylene-*co*-butylene-*block*-styrene), a class of TPE
SST	Total squared variation
S/N ratio	Signal to noise ratio
T_g	Glass transition temperature,
TEM	Transmission electron microscopy
TPE	Thermoplastic elastomer
TPU	Thermoplastic urethane elastomer, a class of TPE
XPS	Photoelectron spectroscopy

1 INTRODUCTION

Hybrid materials can be the specialty material group filling in the gaps between traditional materials [1]. The hybrids, as the name states, are combinations of conventional materials, which are typically form different material groups. As one type of hybrid materials, thermoplastic – metal hybrids have the potential to combine the advantages of both components.

Thermoplastics typically are electrical insulators and have high chemical resistance, but these as many other properties depend on the polymer structure. Most thermoplastics are suited for melt processing and thus offer large freedom in industrial design. In general, they have low modulus and relatively high strength, but their low densities give them good specific mechanical properties. As a group with large variation in structure and crystallinity, a wide range of properties can be obtained, for example in transparency, barrier and surface properties, toughness and stress corrosion resistance. Beside the different property profiles arising from the chemical structure, the properties of thermoplastics can be further varied with fillers and additives. On the other hand, metals have properties that are difficult to reach with polymers, for example high stiffness and thermal and electrical conductivity. Traditionally, it has been easy to design load-bearing applications with metals due to their high strength and strain-hardening capability.

Thus, if these benefits could be combined, the unions of thermoplastics and metals would have attractive property profiles, like electrical conductance and improved corrosion resistance. However the advances come with costs; how we can attain the best and favoured properties of each material without bringing out the negative qualities and additionally, increased complexity and new problems arising from the bonding? Hopefully the answer lies in mechanical design of the structure, and as basis for it, knowing and understanding the underlying phenomena. This governs usability of material in engineering structures as a starting point suitable for different purposes, not just for one or a few specific constructions.

The recent years have seen an increase in the research on hybrids, as well as a rise in the number of industrial products and areas of application. In industrial applications, plastic – metal hybrids are currently used in large sheet constructions, for replacement of welded or machined complicated metallic structures and constructions of small appliances, especially on their casings. Parts for the two latter purposes, and many more, can be produced by insert injection moulding.

As typical to injection moulding, the produced parts are of high accuracy and production rate is high. The benefits of insert injection moulded hybrids include new combinations of material and visual properties, as well as reductions in post-mould assembly operations, weight and expenses, to mention a few. Also, this technique could be used to produce custom solutions by mass-manufacturing methods, as the inserts can be varied, e.g. pre-patterned with evolving printing methods.

On the negative side, reliable adhesion between the material pair is problematic. Little is known about the effect of material properties and material selection on the performance of the hybrids. The early work has been conducted mainly inside companies and academic research has started quite recently (1998, Ramani et al. [2]); thus there is lack of any and especially scientific information on the production and behaviour of plastic – metal hybrids. The recent academic interest on the hybrid structures, combining knowledge from different branches of engineering and science, can thus be seen as a positive sign not only for the development on hybrid materials but also for their industrial implementation.

In this study, the manufacturing and properties of insert injection moulded thermoplastic elastomer (TPE) – metal hybrids are examined. In the theoretical part, several areas important to this study are described. To begin with, hybrids are discussed as a general concept. The thermoplastic – metal hybrids, their merits, drawbacks and processing by insert injection moulding are then reviewed. As a third essential topic to this study, the coupling agent chemistry is introduced.

In the experimental part, two approaches are used: either bonding directly to porous aluminium inserts or bonding to primed stainless steel, copper and aluminium inserts. The different steps in the manufacturing are examined, concentrating on effect of injection moulding and coupling agent application parameters, and linking these to the properties of hybrids and to coupling agent layer formation. Research questions include: how can the injection moulding process affect the hybrid performance? Are other parameters involved? With chemically bonded hybrids, what is the role of the silane interphase and how can it be controlled? And finally, what are the differences between substrates?

The studied metallic materials are stainless steel, copper and aluminium. Steel is commonly used in injection moulded hybrids [3,4,5,6] as inexpensive, high structural strength constituent. Stainless steel, though more expensive, has superior corrosion resistance and lustre and is thus suitable for more demanding applications and visible parts.

Hybrids are also prepared with aluminium [4,6], used in applications where its corrosion resistance and relatively low density are beneficial. Aluminium and its alloys, compared to steel, have also thermal expansion coefficients closer to reinforced plastics, reducing thermal stresses. Copper, to the author´s knowledge, has not previously been used for injection moulded hybrids; it has potential for electrical solutions due to its high conductivity. The other moiety, TPE, has a physically crosslinked structure. This enables melt processing without excluding the rubber elasticity, which gives the low hardness, low modulus of the TPE and thus capability for stress relaxation in hybrid structures.

2 THERMOPLASTIC – METAL HYBRIDS

2.1 Hybrid materials

Hybrid materials are an interesting class of materials. In scientific literature, the concept 'hybrid material' is used for several types of material combinations. In the widest sense it is used for all combinations of two or more materials or of material and space [7]. Some of these hybrids can also be seen simply as structures, or composites, of the constituent materials, depending of the shape and scale of the components. Examples of the variety of hybrid materials include polymeric blends, bi-fibre composites and metal-matrix composites as well as sandwich structures with metal skin plates and polymeric core, and hierarchical inorganic – organic nanostructures. As can be seen from these examples, the concepts ´hybrid´ and ´composite´ are overlapping, but for historical reasons the use of ´composite´ is more restricted.

If following the above definition of ´hybrid´ strictly, also materials like galvanized steel and wood would need to be classified hybrids [7] though they are commonly treated as monolithic materials. So, it is partly a question of convention and partly how the materials are combined: the materials joined after their manufacturing are not considered hybrids [8], nor are coatings or combinations of materials inside one material group. It is, however, considered essential that the combinations should bring properties difficult or impossible to obtain with a single material [8]. Typically hybrids are fusion bonded, i.e. at least part of the structure is formed during processing. However, hybrid materials can also be constructed from blocks with topological interlocking, opening yet new properties arising from the fragmented structure [9]. In this work ´hybrid material´, or ´hybrid´, is used for combinations of different materials, where 1. both components contribute to the bulk properties of the structure 2. at least one of the components is given form and bonded to the other component during the manufacturing.

One reason for the specific role of the hybrid materials compared to monolithic materials are the unique property combinations the hybrids could have, traditionally obtained to some extent with coatings and joined structures. To explore material space for engineering purposes it is common to use material selection charts that show the materials´ positions in property – property space. The materials selection charts can also be useful for exploring the potential of hybrid materials [1]. When a property, such as axial tensile modulus (Young´s modulus) in Fig. 1a is mapped versus density it becomes evident that there are modulus – density regions which could not have been accessed with traditional monolithic materials.

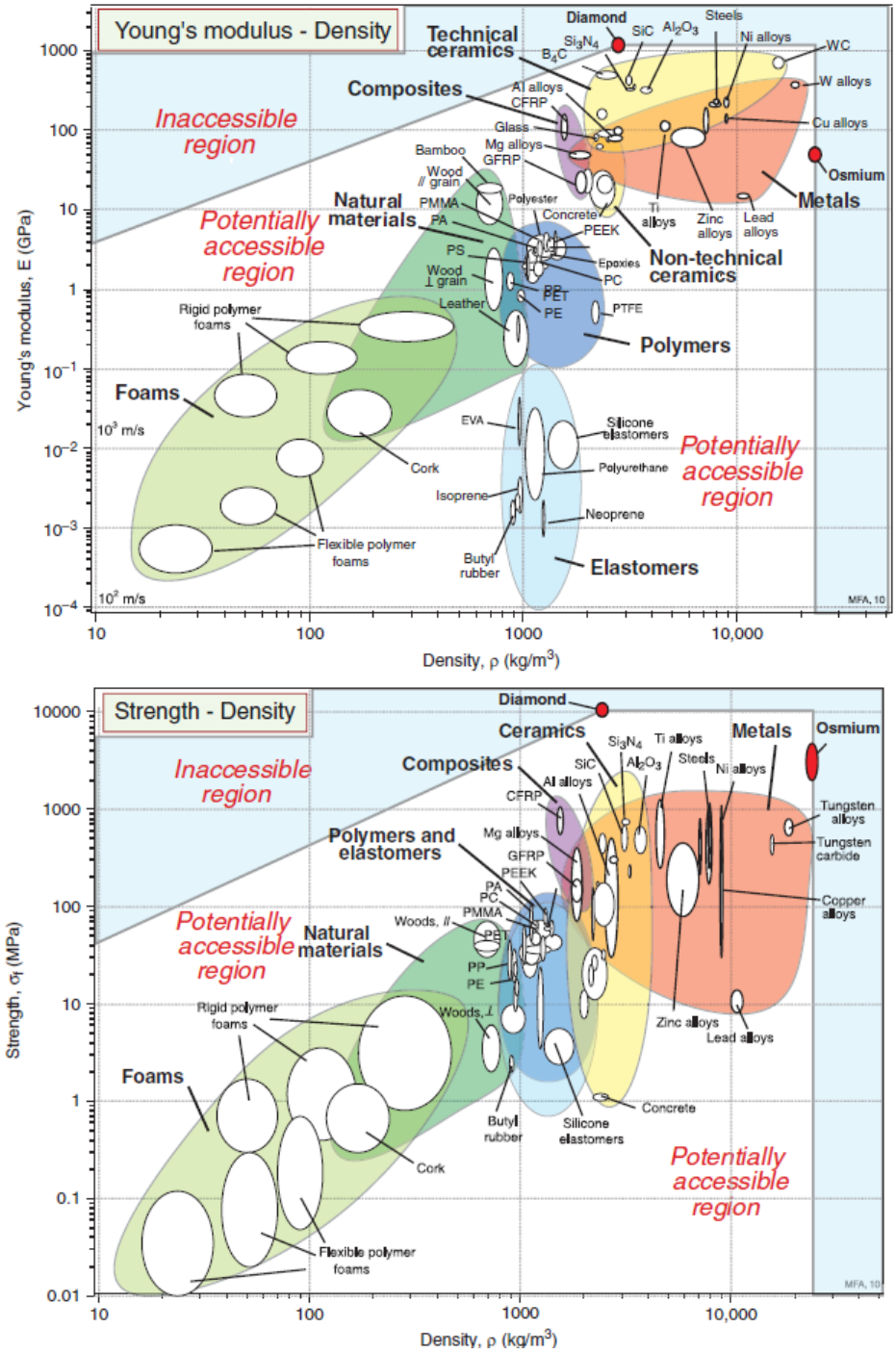

Figure 1. a. Young´s modulus and **b.** strength as function of density [1]. Regions reached with polymers, ceramics and metals are shown, as well as the regions that are theoretically inaccessible. Between these are regions that are theoretically possible to achieve but cannot be reached with current materials.

It has been suggested that, under the physical limits, new property combinations can be accessed by superposition of the currently known materials [7]. For instance, foams, simple combinations of polymeric, ceramic or metallic materials with air, enlarge the low modulus/low density region (see Fig. 1a for polymeric foams) and low strength/low density region (Fig. 1b) we can access. Also, carbon fibre reinforced plastic composites increase both the modulus and strength we can reach with a fixed density. Similarly, at least in theoretical considerations, we can see that new areas in any material selection chart could be entered with hybrid materials [1,7].

It is, however, noted that some properties of monolithic materials are more structure sensitive than others and thus potentially more easy to reach with monolithic material development. For example, while the high modulus and density of metals are inherent to the crystalline structure and quite insensitive to small modifications in the microstructure (structure insensitive properties), the strength and hardness of metals can quite easily be modified by alloying and heat treatments (structure sensitive properties). For example, the strength variation obtainable can be seen in the strength – density chart (Fig 1b), where a metal, for example copper, and its alloys, occupies a range of strengths while the density, naturally, stays essentially constant.

To estimate a quantity obtainable from combinations of materials, theoretical models or semi-empirical equations can be applied. For example the Young´s modulus of unidirectional long fibre – reinforced composite can be accurately estimated by Rule of Mixtures [10] from the moduli of the constituents and fibre volume fraction (f):

$$E_1 = (1-f)*E_{matrix} + f*E_{fibre} \quad (1)$$

This type of weighted means can also be used more generally to give the first estimate of a property of the mixture. Nevertheless, with hybrids, synergetic effects can arise that cannot be attained with monolithic materials. When a synergic effect of a composition is obtained, there is positive (negative) deviation from the Rule of Mixtures level (Fig. 2).

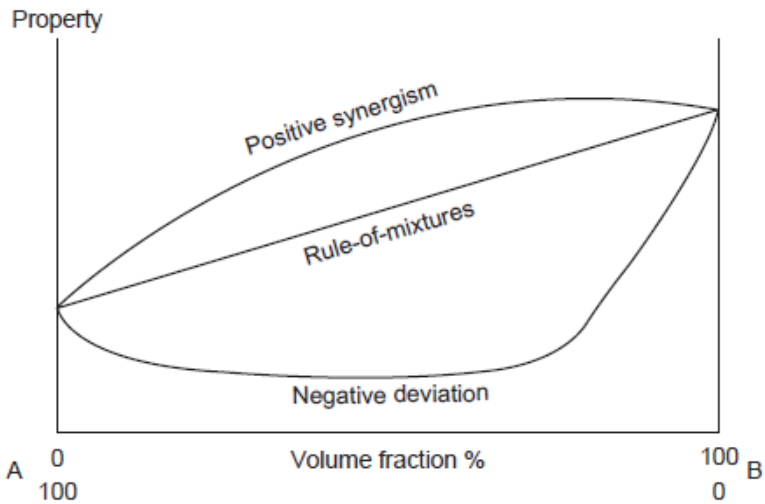

Figure 2. Dependence of a property on volume fraction with or without synergetic effects [11].

Examples of synergetic effects on mechanical properties are seen for example in increased toughness in binary and ternary blends [11]. In the world of plastic – metal hybrids synergetic benefits have been shown to exist, e.g. fibre – metal laminates (FML), layered structures of thin metal sheets and fibre reinforced thermosets, have higher damage tolerance than the individual materials in combination [12]. It is also of interest that biomaterials are rarely monolithic, and producing biomimicking structures could be one area to exploit the hybrid manufacturing technologies.

2.2 Thermoplastic – metal hybrids

Based on the discussion above, there are several types of material combinations that match the concept of thermoplastic – metal hybrids. Such hybrids include e.g. metal filled thermoplastics, polymer coated metal wires, polymer – metal laminates and interpenetrating structures, such as thermoplastic filled metal foams. The following discussion is limited only to macroscopical composites of polymer and metal.

Macroscopical plastic – metal hybrids can be produced, besides injection moulding, directly by extrusion coating and hot-pressing and lamination. However, these are more suitable for producing continuous or 2.5-D structures. Also a new scale in metal coated polymers was presented 2007 by DuPont, based on thick (25…200µm) nanocrystalline metallic coating with untypical coating contribution to mechanical properties, especially in flexure and impact, of the structure [13]. Despite these alternative methods, the insert injection moulding is still mainly challenged by secondary joining in mass-production of complex polymer – metal parts.

At the moment, two main methods in automotive industry that include injection moulding for production of plastic – metal structures are insert injection moulding with perforated inserts for macroscopical interlocking or moulding of thermoplastic component separately and either welding or adhesive bonding to metal subcomponent [14]. Compared to these methods the direct bonding by insert injection moulding offers advantages such as short cycle times, higher structural integrity of the metal part and complex and interfering contact surfaces made possible, and reduced possibility of entrapping air in undercuts [14]. Also, cost savings have been suggested to arise due to high level of part integration, dimensional accuracy of the assembled part, avoidance of warping caused by secondary operations, e.g. laser welding, and integration of plastic and metal processing technologies [8].

Besides the manufacturing and economical benefits, the material properties searched from the individual components include the plastics´

- Design flexibility
- Damping properties
- Chemical and corrosion resistance
- Bulk colouring
- Thermal and electrical insulation
- Weight savings compared to an all-metal counterpart.

And from the metal component

- Structural properties
- Cool touch [6]
- Conductivity
- Impermeability.

As an example, with the TPE – metal hybrids studied here, the main benefits include damping and sealing properties from the elastomer, and structural properties and haptics from the metal constituent. Also each metal studied has it specific benefits, stainless steel corrosion resistance, high stiffness and economical properties/price relationship, OFE-OK copper high conductance, Cu-DHP formability and aluminium light weight and optical properties.

2.3 Insert injection moulding

The multi-material injection moulding includes a variety of techniques, which can be classified e.g. as suggested in Fig. 3. On this division, the three main categories are: multi-component moulding for techniques which use a single-part cavity for one part, multi-shot moulding with two-part cavity or two cavities for one part, and overmoulding techniques using solid preformed inserts [15]. In insert injection moulding the insert can be of any material, including polymers.

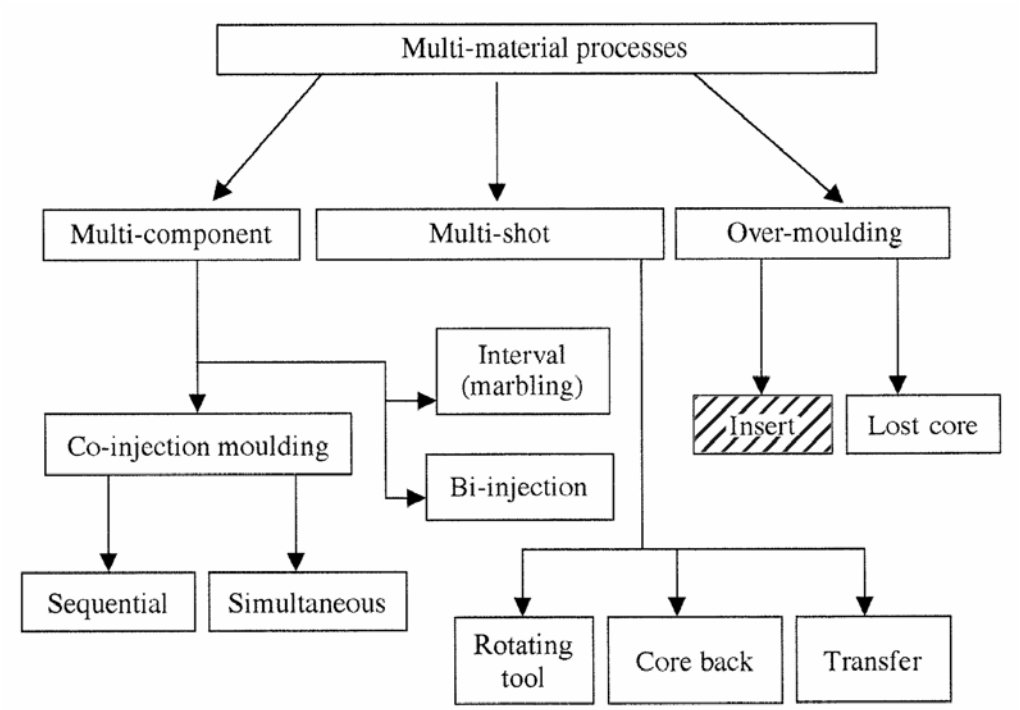

Figure 3. Insert injection moulding related to other multi-material moulding techniques. [15, hatching added].

The main difference between insert injection moulding operation and traditional injection moulding is the automatic placement of inserts in the mould cavities before the mould closure. An insert attachment must be provided; methods include use of vacuum or magnet, gravity, mechanical constraints or pins. Basically the insert injection moulding can be compared to transfer moulding, where the first moulding is moved to another cavity for second injection. At times, instead of insert moulding, term outsert moulding is used, to emphasize that the metal is the defining element, on which or through which smaller objects of polymer are moulded.

However, metal inserts cause several problems in the injection moulding process, due to the different chemical and physical properties of the materials. One of the main problems is related to adhesion between the constituents, as non-modified thermoplastics are not readily bonded to metals due to their chemical nature. In injection moulding the situation is even more complicated since complex melt flow can affect the bonding. General limits cannot be specified for acceptable bond strength as sufficient adhesion is dependent on the part geometry and stresses and environments it is exposed to, as well as expected life time. The life time can differ from higher than or similar to the life times of the constituents to time needed for part assembly. However, in a computational study, it has been shown that for weight reductions the polymer to metal bond strength should be 10MPa or higher for a generic body-in-white (BIW) part [16]. Also, the differences in thermal expansion and the shrinkage of plastic part generate residual stresses leading to e.g. debonding or environmental stress cracking. However, the warpage caused by differences in thermal expansion have been shown to reduce with increments in fibre reinforcement content, simultaneously increasing the Young´s modulus [6].

Yet one specific group of processes exists: it has been suggested several times that the injection moulding pressure can be used for shaping metallic inserts [17,18,19]. This is comparable to well-established in-mould labelling with polymeric film inserts, where the film insert can be partially stretched during the moulding cycle. There are at least two industrial techniques in this field, i.e. Polymer Injection Forming and Polymer Injection Compression Forming by Tata Steel (former Corus) [19].

2.4 Chemical and micromechanical adhesion in injection moulded hybrids

Adhesion in injection moulded plastic – metal hybrids can be obtained in several ways. Macromechanical anchoring through perforations is used in industrial solutions (for example [5,20]). Also, geometries where shrinkage leads to tightening of plastic around the insert can be used when product design allows it (e.g. [21]). An advantage specific to components with adhesion obtained purely by mechanical interlocking is the recyclability of the structure, as the plastic – metal bond can be eliminated by hammer crushing [5]. Besides these macroscopic interlocking methods, so called direct bonding technologies are established and the demonstrated methods can be categorized to: [22]

- Micro-scale mechanical interlocking
- Metal priming
- Chemical modification of the thermoplastic
- Other.

If excluding the thermoplastics modification and macromechanical anchoring, several solutions has been suggested based on either micromechanical anchoring to surface irregularities and cavities, or use of primers. Also surface activation e.g. by plasma is used, but often as part of a surface preparation protocol including several steps.

One of the first academic studies was conducted on moulding of polycarbonate (PC) – aluminium or PC – steel macrocomposites with a butt joint [2]. The main provision for successful manufacturing was preheating of the insert [2]. In this early study the effect of moulding parameters was already considered. The tensile strength was dependent on the surface temperature of the insert and the interaction of surface temperature, screw linear movement speed, i.e. injection speed and thickness of PC layer [2]. The combination of high surface temperature, high screw speed, thin polymer layer and high hold pressure gave highest tensile strength 38.5±9.9MPa [2]. The increase in strength was thought to derive from the decrease of melt viscosity, leading to better penetration to insert microcavities [2].

Later, the effect of surface roughness has been studied with overmoulding of glass-fibre reinforced polypropene (PP) and polyphenylenesulphide (PPS) on oven-heated aluminium [23]. With glass-reinforced PP, the difference between studied surface roughnesses, 2µm or 6µm (R_a), was not enough to affect the shear strength of the bond, but did increase the fraction of polymer residual on the metal failure surface [23]. However using higher glass-fibre loading in PP increased the shear strength [23]. Glass-reinforced PPS was also tested to enable high adherend temperature up to 450°C and thus lower the polymer melt skin viscosity. With this material, increase in surface roughness augmented the shear strength but the highest strength obtained (0.97±0.02MPa) [23] is still quite modest.

Three-component structures have also been prepared by moulding a TPE interlayer between plasma-treated metal and thermoplastic inserts [24]. Preheating of the metal insert increased adhesion in these structures [24] as well as in production of hybrid gears [25]. The hybrid gears had a (polyamide 66 / poly(phenylene oxide)) blend layer moulded over metal (steel or stainless steel) core, a design that combines the stiffness of the metal and the tribological properties and noise reduction capability of the plastic [25]. In moulding of the gears, without metal preheating no adhesion was obtained and the plastic part cracked soon after moulding [25]. The used preheating temperatures, 230–250°C were high compared to melt temperature, 270–290°C [25].

An alternative to preheating is to use chemical coupling agents. Boerio et al. [3] studied the bonding of injection moulded polyvinylchloride (PVC) to aminosilane (γ-aminopropyltriethoxysilane, γ-APS, or γ-aminoethylaminopropyltrimethoxysilane, γ-AEAPS) treated steel substrates. After moulding the PVC – steel hybrids were annealed in oven at 170°C (i.e. close to moulding temperature) for 10–30min, resulting in 90° peel strength on the order of 30–40 N/cm [3]. Based on analytical studies, polymer – silane bond mechanism was suggested; this is further discussed in Chapter 3.3. Another example of coupling agent bonded insert injection moulded hybrid is embedded structure of NiTi shape memory alloy in polyamide 6 matrix [26]. Out of several surface treatment protocols, highest NiTi ribbon pull-out strength (9MPa) was obtained after a combination of mechanical polishing, plasma treatment, application of coupling agent and a second plasma treatment [26].

Besides coupling agents, also polymeric primers, notably thicker than chemical primers (micrometers vs. a few monolayers), have been studied in injection moulded hybrids, for example with simple overlapping panels and U-form hybrid structures [27]. Also a commercial procedure for moulding an object directly on amine treated metal sheets by injection moulding exists for polybutyleneterephthalate (PBT) and PPS from Taisei Plas [28]. The bonding here is claimed to be based on microscale interlocking and partially on exothermic reactions, either between the amine and ester moiety of PBT or the amine and chlorineted polymerization residuals of PPS [28].

Despite most solutions include moulding of the plastic on the metal insert, also inversed sequence processes exist. A recent process combines injection moulding with die casting of metal for production of plastic parts with electrically conductive paths [29]. In this approach, a heat resistant thermoplastic is moulded first followed by casting of low melt temperature (96–200°C) alloy [29].

3 SILANE COUPLING AGENTS

Classically, a coupling agent is defined as an adhesion promoter that forms covalent bonds with two components of a structure, usually the inorganic and the organic part [30,31]. Organosilanes are commonly used as coupling agents in glass fiber reinforced composites to improve the bonding between glass fiber and thermoset matrix and also as surface treatment on metal surfaces to suppress corrosion of the underlying substrate. For bonding applications, typically used organosilanic coupling agents have structure of $(R_1O)_3Si–(CH_2)_n–X$, where R_1 is an alkane and X is a functional group. The alkane linker between the silicon atom and the functional group has typically length of n = 2 or 3 [31]. The organofunctional moiety, X, is chosen to be compatible with the polymer for example in polymeric coatings, paints and adhesives. Typical reactive groups include epoxy, amino, ester and vinyl functionalities. Bond strength, especially in humid environments, and corrosion resistance can be improved by the choice of silane functionality, and additionally, by silane treatment conditions. Also other silane backboned molecules, for example bis(alkoxysilyl)alkanes, and other organometal complexes, like titanates [30], are used.

3.1 Reactions in aqueous solutions and on mineral surfaces

Silanes are typically applied from low concentration aqueous solutions. The favoured reactions taking place are [e.g. 30,32]:

The *hydrolysis* of the alkoxy groups in water resulting in formation of *silanols*

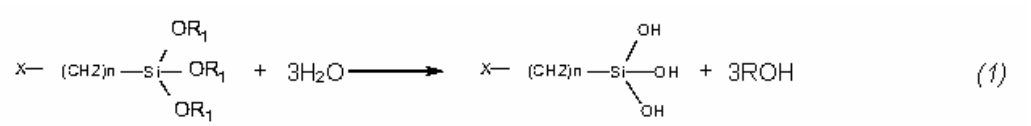

Condensation and *reactions with the hydroxyl groups* at the surface, forming covalent metal–oxygen–silicon, i.e., metalloxy bonds.

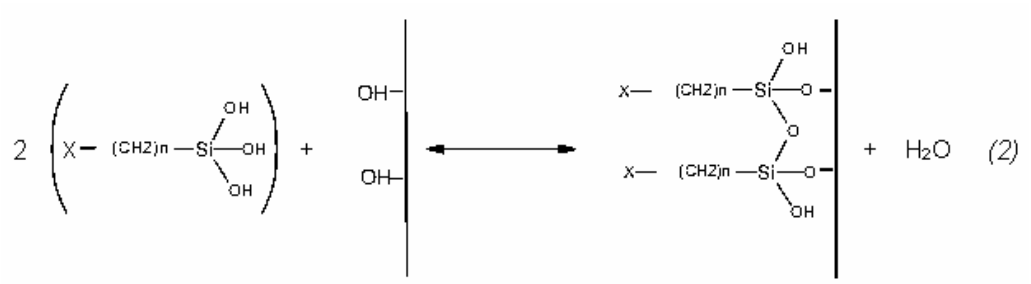

The properties governing the application of silanes are solubility to water or water/alcohol solutions and rate of hydrolysis and condensation. The hydrolysis rate depends primarily on the chemical structure: the shorter the alkoxy group the greater the reactivity, i.e. propoxy<<ethoxy<methoxy [32] and secondarily on the pH of the solution: at neutral pH the rate is lowest (Fig 4., right) [32]. Also the organic group and length of the alkane linker affect the hydrolysis, possibly through the solubility [32]. The formed silanols are generally most stable at around pH 3, and begin to condensate to oligomers at higher or lower pH (Fig.4, left). The reaction (2) with the hydroxyl-bearing surfaces takes place in two steps: hydrogen bonding followed by elimination of water, leading to covalent bond formation. The competing condensation reactions can cause oligomerization of the bonded silanols, thus leading to a deviation from the theoretical coverage of the surface. However, the condensation is partially suppressed by using low concentration solutions: the typical concentration range is 0.01…2% [33]. Silane layers in practise consist of partially physisorbed molecules; it has been estimated that commercial glass fibre sizing consists of 10–20 silane monolayers [34].

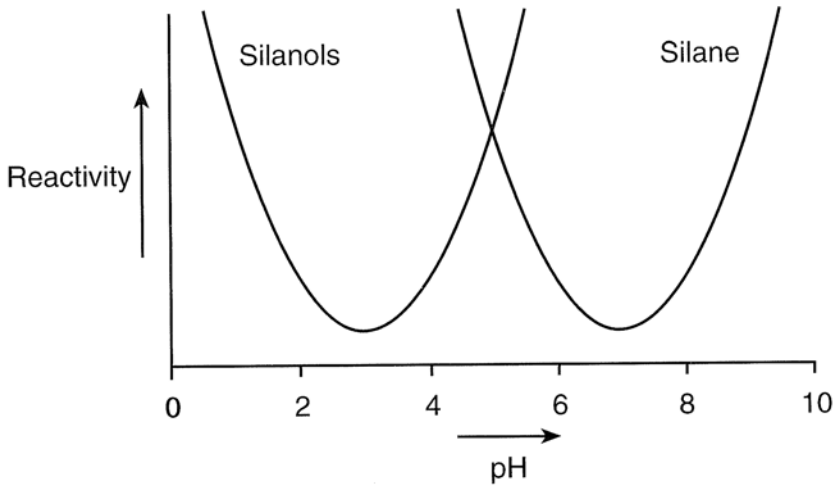

Figure 4. The sensitivity of silanes towards hydrolysis and silanols towards reactions with hydroxyl groups as function of pH [32].

Aminofunctional silanes have high solubility to water at alkaline conditions and hydrolyse rapidly [34]. Hydrolysed γ-APS may form hydrogen bonded rings, protecting them from condensation [32,34]. In acidic solutions γ-APS, contrary, protonates and forms zwitterions at pH range of 3–6 [34]. However, for aminosilane bonded structures, unexpectedly low performance has been observed compared to unsilanized references, for example decrease of bond strength in humid environment for epoxy – γ-APS – mild steel [35] or an increase in water absorption for the similar system [36], both with γ-APS deposited from alkaline pH.

The deposition of γ-APS on metal surfaces has been studied in detail and it has been shown, that the protonation of the amino-group can lead to up-side down bonding of the amine on the metal surface through hydrogen bonds [34,35,36,37], instead of covalent bonding to metal. This has a strong influence on the silane layer properties [35,38,39] leading to the described poor performance after water absorption due to hydrolysis of the amine – steel bond [35,36]. However the results of environmental tests are partially uncomplimentary, since for epoxy – γ-APS – mild steel coating with γ-APS deposited from pH of 10.5, the wet adhesion strength has been reported to be lower [35] or greater [36] than with unprimed mild steel. On the other hand, the adhesion of γ-APS primed carbon steel coated with polyurethane modified alkyd or alkyd coating after immersion to 0.6M NaCl (aq.) was equal to or greater than of unprimed carbon steel [40]. The use of γ-APS primer did not however reduce the cathodic disbonding rate, contrary to γ-APS primed carbon steel with epoxy coating [40]. This was explained by two degradation mechanisms, in the case of epoxy coating by disruption of interfacial bonds between polymeric coating and the substrate and with alkyd coatings of direct degradation of the coating [40]. Thus the silane behavior is not the limiting factor in all circumstances.

3.2 Thickness and structure of the coupling agent layers

The optimum thickness of the coupling agent layer depends on the materials to be bonded. In fibre reinforced composites the finely divided reinforcements surrounded by matrix require only few monolayers of the silane coupling agent at the surface for chemical modification [34], whereas massive structures need a thick hydrolysed silane layer that can compensate for mechanical stresses and possibly have a solvent effect for the matrix [34].

The silane thickness determination is based on several analytical techniques, most popular one being ellipsometry (e.g [43,44,45]). Also indirect quantification of the layer thickness is often used, for example based on XPS signal intensity relationship calculations [46,47] or gravimetric techniques [48,49]. Regrettably, these all are more or less averaging techniques and ellipsometry is suitable only for certain materials and thicknesses. On the other hand, microscopical techniques would give direct information on the thickness distribution and layer morphology. There are a few such examples of cross-sectional microscopy [42,43] but the larger application has been hindered by the lack of suitable sample preparation techniques, mainly due to different hardness of metal and silane layers and the silane layer reactivity.

The thickness of the formed silane layer depends strongly on the used solution concentration but it is almost independent of the dipping time of the substrates into the solution [41]. Effect of silane bath concentration have been studied for many systems, e.g. according to Chovelon et al., deposition of γ-APS on stainless steel surface followed by rinsing step led to increase in the film thickness up to silane concentration of 0.3%, and decrease in the film thickness with higher silane concentrations [39]. When the silane concentration exceeded 0.3%, it was suggested that defect formation and perturbation in the organization of the silane film takes place and during a washing step weakly bonded silane layers are washed out [39]. However in a study of bis-1,2-(triethoxysilyl)ethane by De Graeve et al. low concentration led to formation of a less compact layer [42]. In the study of Chovelon et al., the thickness determination was based on relative signal intensities of Low-Energy Electron Induced X-ray Spectrometry and in the study of De Graeve et al. by examining liquid nitrogen fractured samples with field emission scanning electron microscope (FESEM), enabling the estimates on the morphologies of the layers [42].

The silane layer formation is also dependent on the metal surface microstructure. The effect of the underlying substrate has drawn little attention and has been mainly studied with aluminium alloys [50,51]. The classical theory assumes that silanes arrange themselves perpendicular to the metal surface forming a silane monolayer, but in practice the silane adhesion promoter consists of several layers [32,34]. Petrie has suggested that rough substrate surface can break up the order in the of the first silane layer and therefore obstruct the formation of the second layer, and draws a conclusion that smooth surfaces are the best substrates for silane layer formation [33]. However, neither analytical nor modelling evidence has been presented to either support or reject this view. Also, the scale or irregularity of the surface roughness sufficient to contribute to this effect has not been consirered.

Jussila et al. studied the mechanisms of γ-APS bonded to oxidized stainless steel surfaces with different concentration of hydroxyl groups at the surface [52]. With low concentration of the hydroxyl groups, the number of metalloxy bonds was low and silane was suggested to have free silanol groups, leading to silane cluster formation by silane polymerization [52]. On the other hand, when the stainless steel surface had high number of hydroxyl groups the γ-APS adsorbed mainly as isolated monomers, resulting a monolayer with high degree of silane to metal bonding [52]. Deflorian et al, targeting for multimetal priming, studied γ-glycidoxypropyltrimethoxysilane (γ-GPS) on copper and Mg alloyed aluminium [53]. The silanization procedure used for aluminium led to uneven silane layer on copper [53].

3.3 Bonding with polymers

The definition (p.13) of a coupling agent implies that it should form primary bonds both with the substrate and with the polymer [30]. However this does not always apply as also secondary bonding with the polymer takes place. Several mechanisms contributing to the polymer – silane bonding have been suggested.

Covalent bonding. The chemical bonding has been demonstrated e.g. for PVC bonding on steel using γ-APS or γ-AEAPS as coupling agent. The latter provided higher interaction with PVC, as monitored by XPS measurements of the concentration of chlorine residual on the metal side after peel testing [3]. Based on XPS and FT-IR studies, the suggested polymer – silane bond mechanism is the reaction of amine with allylic chloride formed in the thermal degradation of PVC [3]. This was further studied with a partially dehydrochlorinated PVC interlayer between γ-AEAPS and PVC, which confirmed that the formation of allylic chlorides was the rate limiting step [3]. Other examples of thermoplastics – silane pairs with covalent bonding, as listed by Plueddemann, include styrene-maleic anhydride copolymer – epoxyfunctional silane, polyethylene – vinylsilane and polyolefin – azidofunctional silane pairs, the two last ones at moulding temperatures [34]. However, for majority of thermoplastics there is no certainty of chemical reaction between the polymer and the silane [34].

It has been shown for thermoplastics –silane pairs which cannot form covalent bonds that the bond strength reaches the maximum when the solubility of the silane and polymer meet [34], indicating bonding by *interdiffusion* and possibly by *chain entanglement*. The bonding by interdiffusion and chain entanglement is the most effective in the case of amorphous polymers [34]. Considering the adhesion purely by interdiffusion as classified by Chaudhury et al., either no interdiffusion takes place and a sharp interface is formed, or the interdiffusion of the primer and polymer chains leads to formation of an interphase, or after interdiffusion an interpenetrating network is formed [54]. The first one leads to poor adhesion, dependent on the wetting of the surface by the polymer, whilst the last can ideally have strength comparable to or greater than the cohesive strength of the polymer [54]. The interphase formation has been confirmed directly at least by XPS depth profiling [54] and secondary neutral mass spectrometry [55].

In the case of PVC – γ-AEAPS pair discussed above, the bond strength depended also on the extent of polymer – silane interdiffusion [3,54]. Low precuring temperature of the silane led to greatest interdiffusion and high bond strength with cohesive failure [3,54]. However the relative loss of adhesion after water immersion was greatest for uncrosslinked silane, and negligible for samples cured at high temperatures, which failed interfacially between the silane coating and PVC [54]. Similarly for polystyrene – γ-AEAPS pair, polymer – silane interphase forms when γ-AEAPS is uncrosslinked prior to polymer bonding, and crosslinking reduces the interphase thickness [55].

Other mechanisms of interest include formation of an *interpenetrating network* (IPN) [30] or a *porous polysiloxane layer* that can help the polymer to mechanically interlock to the substrate [33]. At least in two cases it has been speculated that the silane acts as a solvent for molten thermoplastic and forms an IPN after cooling down [34]. Further support to the contribution of IPN formation is the adhesion obtained by unfunctionalized orthosilicates such as tetraethyl orthosilicate, $(R_1O)_4Si$ [31]. It has been postulated that the coupling effect of orthosilicates is based on to hydrolysis to oligomers, interdiffusion with polymer and formation of an IPN [31].

3.4 Other actions addressed to coupling agent layers

Also several other actions beside adhesive properties have been addressed to coupling agent layer, many considerations done from mechanical point of view. These include coupling agent working as an intermediate modulus layer or plastically deformable layer relieving the stresses between inorganic and organic part [30,31]. The stress-relaxation by reversible hydrolytic bond relaxation in humid conditions [30,31] has also been suggested. The possible actions as oxide reinforcement [30] and causing preferential orientation to the polymer layer [31] have also been mentioned.

The silane coupling agent layers can also have corrosion inhibitive properties [56]. These can be reached either with non-reactive silanes or by adding inorganic or organic inhibitors to silane layers [56]. Several silanes with inhibitive properties have been reported with structure of $(R_1O)_3Si(CH_2)_n–Y–(CH_2)_n(OR_1)_3$, from bis-1,2-(triethoxysilyl)ethane [38] with alkane backbone to bis-(3-(trimethoxysilyl)propyl)amine [57,58] and bis-(3-(triethoxysilyl)propyl)tetrasulfides with heteroatom backbones [57]. Mixtures of the two last ones have shown better corrosion resistance compared to individual components as the hydrophilicity of bis-amine leads to even layer formation while the hydrophobicity of bis-sulfur is beneficial for corrosion protection [57]. The inorganic particles incorporated in the bis-silane layers that contribute to corrosion protection range from cerium nitrate [59] to silica micro- and nanoparticles [60,61].

4 AIMS OF THIS STUDY

Hypotheses behind this work are:

1. Thermoplastic material can be bonded to planar metal insert by injection moulding without insert preheating or post-mould thermal treatment
2. Adhesive strength of such hybrids is suitable for practical applications
3. The adhesion of such hybrids could be realised via three methods: micromechanical bonding, use of chemical coupling agent or use of low modulus polymeric interlayer. The two first approaches are studied in this work, and the structure studied here could act as an elastic middle layer itself.
4. The performance of the injection moulded hybrids is affected by the processing parameters
5. The bonding depends on the properties of the interfacial layer (coupling agent layer), which is itself dependent on the substrate surface state.

The overall objective of this work is to study alternative processes to insert preheating or use of perforated inserts. This goal is searched in the Publications I-VI, supported by some unpublished data. The effects of injection moulding parameters on adhesion in micromechanically bonded hybrids are studied in Publications I–II. The properties of coupling agent layers and linkage of these to the performance of the hybrids are studied in Publications III–V for stainless steel and copper with different surfaces modifications. Aluminium as substrate material is described in Publication VI, which concentrates on environmental resistance of chemically bonded hybrids with selected substrate materials.

5 EXPERIMENTAL PROCEDURES

The studied hybrid materials were layered TPE – metal structures, manufactured directly by insert injection moulding. Two approaches were used for obtaining a bond strength adequate for practical applications: surface etching to increase the surface roughness for micro-scale interlocking ("micromechanical bonding") and bonding to metal surface treated with chemical coupling agent ("chemical bonding").

Two set-ups were used for injection moulding. In the beginning, Mould I was used for micromechanically bonded hybrids. Later on, Mould II was used for both types of hybrids. Structure and dimensions of the studied hybrids are depicted in Fig. 5.

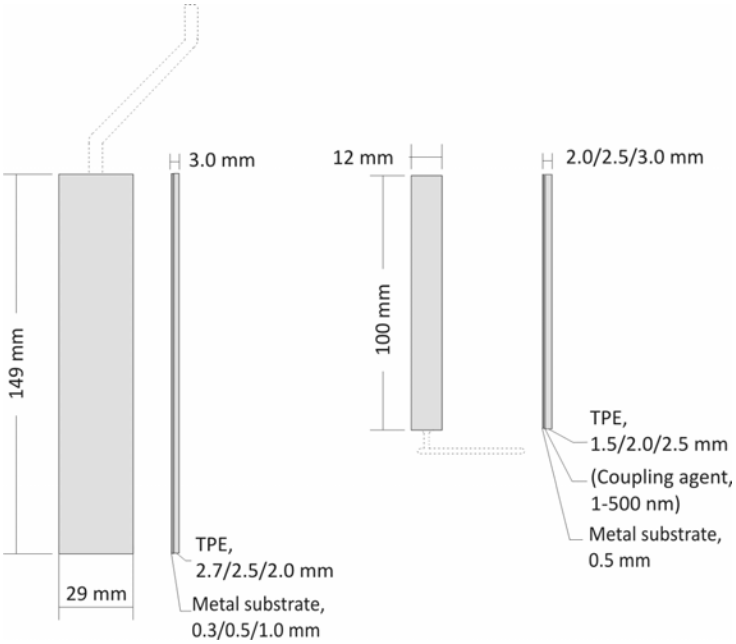

Figure 5. The structure and dimensions of the hybrids manufactured with Mould I (left) and Mould II (right). The mould channel location is shown in dashed line.

5.1 Substrate materials and treatments prior moulding

Hybrids with micromechanical bonding

Aluminium sheets, grade 1050, min. 99.50% Al [62], were obtained from Tibnor. Three sheet thicknesses, 1.0mm, 0.5mm and 0.3mm, were used in Publication I and 0.5mm in Publication II. The sheets were cleaned with ethanol and acetone, pre-etched in 5%NaOH for 5 min, desmutted in 30%HNO_3 bath and rinsed with water. This was followed by P2 etching [63] for 10 min with stirring at 65…68°C, according to ASTM D 2651-90. After etching the sheets were rinsed with water and dried at 60°C.

Hybrids with chemical coupling agent

OFE-OK copper, DHP copper, stainless steel and aluminium alloy in sheet form with thickness of 0.5mm were used as substrates. The substrate materials, their surface treatments and the surface structures formed are described in Table 1. All substrates were degreased with acetone and ethanol in an ultrasonication bath (3 min + 3 min), followed by polishing and oxidation treatments when applicable. Stainless steel was polished industrially, while the copper substrates were polished in the laboratory. Degreased as-received substrates were used as reference for modified copper (Publication V) and stainless steel (Publications III-IV).

Table 1. Substrate materials and their surface preparation.

Substrate	Composition	Surface preparation	Effects of surface preparation	Publication
OFE-OK copper (Luvata)	Cu ≥ 99.99%, O_2 ≤ 5 ppm	As-received	Degreasing	V
		Electrolytical polishing	Even surface, thin native oxide of Cu_2O and CuO [64,65]	V, VI
		Electrolytical polishing + 25 min at 200°C in air	Formation of Cu_2O layer, thickness 30nm	V, VI
DHP-Cu copper (Luvata)	Cu ≥ 99.90%, P 150–400 ppm	As-received	Degreasing	V
		Electrolytical polishing	Even surface, thin native oxide of Cu_2O and CuO [64,65]	V
		Electrolytical polishing +25 min at 200°C in air	Formation of Cu_2O layer, thickness 30–40nm [66]	V
AISI 304 Stainless steel (Outokumpu Tornio Works)	Cr 18.20% Ni 8.20% C 0.05% Mn 1.70% Si 0.53% P, S < 0.1% Fe rem.	As-received: cold-rolled, heat-treated, pickled, skin passed	Degreasing	III, IV
		Electrolytic polishing	Even surface, thin native oxide	VI
		Electrolytic polishing+ 5 min at 350°C in air	Formation of thin M_2O_3 layer with islands [67]	III, IV
		Electrolytic polishing+ 100 min at 350°C in air	Formation of M_2O_3 layer, thickness 15nm [67]	III, IV, VI
AlMg3 (5754) aluminium alloy (Tibnor)	Mg 2.6–3.9% Si ,Fe 0.40% Mn 0.50% Cr , Cu, Zn, Ti ≤0.3% Al rem. [62]	Etching 5 min in 5%NaOH, rinse in 30% HNO_3 and H_2O	Formation of high surface roughness oxide layer	VI

After the metal surface preparations the silane coupling agent, N-(β-aminoethyl)-γ-aminopropyltrimethoxysilane, γ-AEAPS (Dow Corning Z-6020) was applied. Three application methods were used: spraying, brushing or dipping in dilute silane solution for 5 min, from which the last one is used if not otherwise stated. The concentrations of silane solutions (0.1, 0.25, 0.5 and 1.0%) used are volume fractions of aqueous solutions. Also thinning of the uncured silane layer by dipping to ion-exchanged water for 1 min was tried. Prior the application the silane solution was stirred for 1h for hydrolysis and the silanized substrates were crosslinked at 110°C for 10min.

5.2 Hybrid manufacturing

Hybrids with micromechanical bonding

Commercial poly(styrene-*block*-ethylene-*co*-butylene-*block*-styrene) (SEBS, Kraiburg Thermolast K TG7MGZ) was used for injection moulding. Such TPEs are phase-separated tri-block copolymers with a structure of styrene-diene-styrene, where the styrene segments contribute e.g. to stiffness and the diene segments give rise, inter alia, to high elongation and softness [68]. The grade used was adhesion modified for multi-shot injection moulding applications.

Two set-ups were used for this study. Mould I (Publication I) was used on a Krauss-Maffei 80-220/60/90 CZL injection moulding machine vertical B-unit (clamping force 800 kN, p_{max} 2400 bar, screw diameter 18 mm). A rectangular gate (1x6 mm) was located at the short edge of the 3 mm thick cavity. The aluminium inserts were fixed at the rear mould side with double sided tape. Injection moulding parameters are as shown in Table 2. As inserts with thickness of 0.3, 0.5 and 1.0 mm were used, the shot volume was varied according to the insert thickness (free cavity volume).

Table 2. Moulding conditions for SEBS

Parameter	Value
Injection speed	15 mm/s
Mould temperature	70°C
Hold pressure	450 bar, 8 s
Cooling time	30 s
Plastization	100 rpm, 10bar
Cylinder temperature	250–240–230–190°C
Material predrying	80°C, 2 h

Mould II (Publication II) was used on a Fanuc Roboshot αC30 injection moulding machine (clamping force 300 kN, p_{max} 2000 bar, screw diameter 20 mm). The steel two-plated mould has interchangeable mould inserts for different cavity depths: cavity depths of 3.1, 2.6 and 2.1 mm were used. The metal sheet thickness was kept constant at 0.5 mm. A fan

gate (0.5x5 mm) was located at the short edge of the cavity. The back mould was heated with electrical heating cartridges and temperature controlled via a thermocouple near the back mould surface. Oil tempering was used in the front mould, leading to small temperature differences between the mould sides, dependent on the temperature setting and leading to a higher temperature on the back mould side. The inserts were fixed to back mould side with vacuum prior to closure of the mould.

Hybrids with chemical coupling agent

The polyester-based thermoplastic urethane (TPU) grade was commercial Estane GP 85 AE nat for injection moulding applications. Thermoplastic ester-based polyurethanes such as Estane consist of three components: di-isocyanate (methylene 4,4´-diphenyl di-isocyanate, MDI), 1,4-butanediol as chain extender and polyol [68,69]. The first two form the hard segments and the polyol the flexible soft segment.

Table 3. Moulding conditions for TPU

Parameter	Value
Injection speed	20 mm/s (fill time 1.1s)
Mould temperature	50°C
Hold pressure	750 bar, 3 s
Cooling time	15 s
Plastization	50 rpm, 10–30 bar
Cylinder temperature	200–195–190–185°C
Material predrying	80°C, 3 h

The hybrid specimens were injection moulded with a Fanuc Roboshot αC30 machine using Mould II with a cavity depth of 2.6mm. The moulding parameters are given in Table 3. Part of the inserts was not silane treated to provide a non-bonded gripping area for peel tests.

5.3 Characterization of metal substrates and silane coatings

Hybrids with micromechanical bonding

A scanning electron microscope (SEM) (Philips XL30) was used to study the surface of aluminium substrates.

Hybrids with chemical coupling agent

The metal substrates and silane coatings on the substrates were imaged by optical microscopy (OM, Leica DM 2500 M), FESEM (UHR FESEM Zeiss ULTRAplus) and transmission electron microscopy (TEM, Jeol JEM 2010). In initial testing of silane application conditions, contact angle measurements were done with 5 µl drops of MilliQ (18.2 MΩcm) water and the sessile drop profiles recorded with a goniometric system (Photocomp, Finland).

The silane layer thicknesses were determined from scalpel fractured silane layers with FESEM, and supplementary data obtained from conventional cross-section TEM studies. The surface topography and the average surface roughness were determined by atomic force microscopy (AFM, NanoScope E AFM/STM). Scanned areas were 2 µm x 2 µm for imaging and 13 µm x 13 µm for surface roughness determination.

Additionally, the copper substrates and silane layers on copper substrates were characterized with reflection absorption infrared spectroscopy (RAIRS, Bruker Optics Tensor 27 with variable angle Veemax II reflection unit from Pike Technologies). The angle was 70°, scan number 128, resolution 4 cm^{-1} and sample size 25 mm x 30 mm. the background spectrum was collected with a gold-plated mirror.

5.4 Characterization of plastic – metal hybrids

Hybrids with micromechanical bonding

180º peel testing was used to determine the adhesive strength. Modified method based on ASTM D 903 – 98 was used with evident changes in the sample preparation and dimensions. Prior testing the samples were stored at 23°C and 50 ± 2 % relative humidity (%RH) for minimum of 48 h and maximum of 120 h. A universal mechanical testing machine with 1 kN load shell (Messphysik, Austria) was used with a cross-head speed of 100 mm/min. The test specimens were opened manually, from the end of the cavity, opposite to the gate. SEM was used to study the SEBS and aluminium fracture surfaces of the hybrids after peel testing (Publication I).

Hybrids with chemical coupling agent

The adhesion of TPU – metal hybrids was determined similarly to the SEBS hybrids, with the non-silanized area placed at the end of the cavity. After peel testing, the fracture surfaces were studied by optical stereomicroscopy (Leica MZ 7.5, image analysis with ImageTool 3.00 for determining fraction of cohesive failure area), SEM and additionally by dark field OM (Leica DM 2500 M). The chemical composition of the peeled sample surfaces was studied with Fourier transform infrared spectroscopy (FT-IR): the measurements were done either in attenuated total reflection (ATR) (Publication III) or in reflection-absorption for metal sides (Publications V and VI). For ATR a GladiATR (Pike Technologies) with diamond crystal was used with scan number of 64. For RAIRS the mask size was 3/8” (sample size 100 mm x 11 mm) and angle 40° (Publication V) or 70° (Publication VI), otherwise the device and parameters were as given in Chapter 5.3.

The environmental resistance of TPU – metal hybrids was evaluated by exposure to isothermal (500h at 85°C/ambient atmosphere), isohume (500h at 25°C/85%RH) or hygrothermal conditions (500h at 85°C/85%RH). Related changes in thermal, chemical and bonding properties and microstructure of the hybrids were examined. The thermal properties of the TPU were studied by differential scanning calorimetry (DSC), using a Netzsch DSC 204 F1 with liquid nitrogen cooling. The tests were performed under nitrogen flow and the scanning program was: cooling to -100°C, heating 20°C /min up to 220°C (1st heating) followed by re-cooling to -100°C and repeating the heating cycle (2nd heating). The chemical composition was studied with ATR FT-IR and the microstructure of the hybrids with FESEM.

5.5 Graphical summaries of the experimental steps

Hybrids with micromechanical bonding

The schematic process chart for SEBS – aluminium hybrids is shown in Fig. 6.

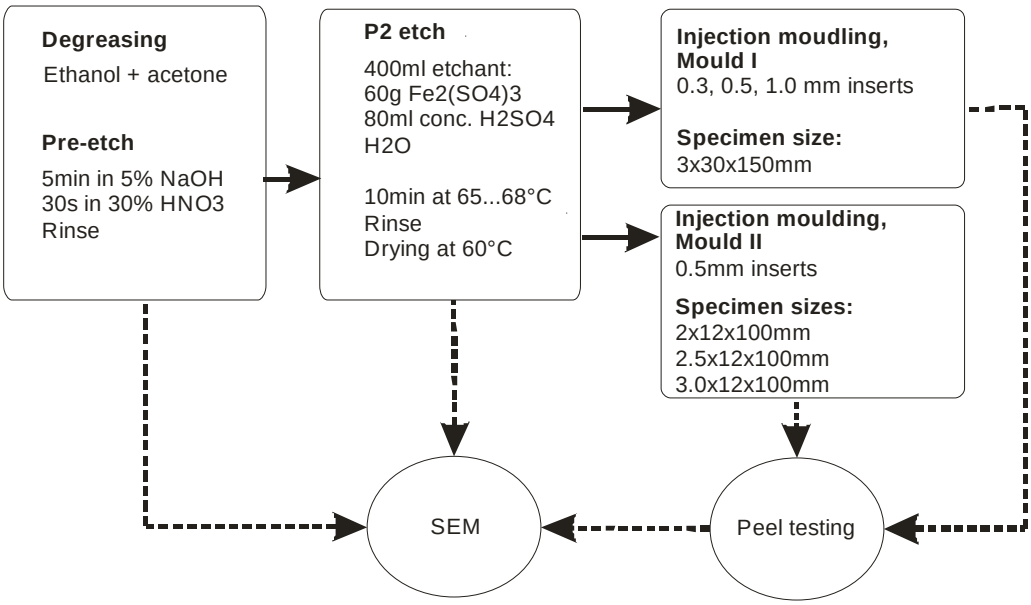

Figure 6. Manufacturing and characterization of SEBS – aluminium hybrids.

Hybrids with chemical coupling agent

The schematic process chart for TPU – γ-AEAPS – stainless steel/copper/aluminium hybrids is shown in Fig. 7. The cross-references to Publications and full experimental array for each substrate material are collected to the Appendix of this work.

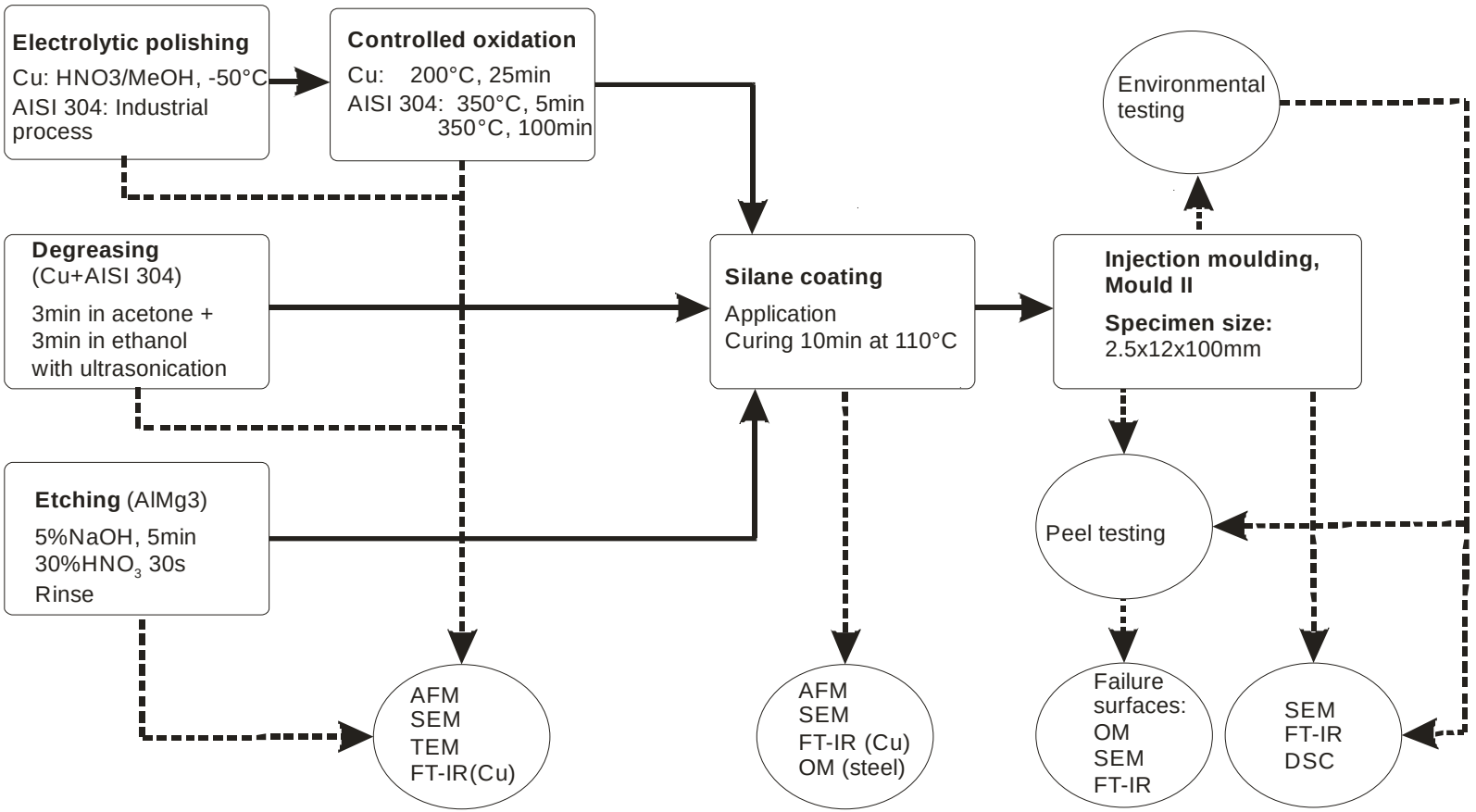

Figure 7. Different steps in manufacturing and characterization of TPU – γ-AEAPS – metal hybrids.

6 RESULTS AND DISCUSSION

6.1 Injection moulding

The first type of hybrids, SEBS bonded micromechanically to porous aluminium surface, was used to demonstrate the manufacturing method, to study the influence of moulding parameters and effect of polymer/metal thickness ratio.

SEBS overmoulding on P2 etched aluminium resulted in a peel strength of 9.3 N/cm. The failure was partially cohesive in SEBS but stayed close to the TPE – metal interface. Without P2 etching, the adhesion to NaOH pre-etched aluminium is weak and without any etching (degreased aluminium) no measurable bonding is obtained.

Two approaches were used to study the effect of polymer/metal thickness ratio. First, inserts of thickness of 0.3mm, 0.5mm and 1.0mm were overmoulded in a cavity of 3mm (Mould I). Atferwards, 0.5mm thick aluminium inserts were overmoulded with cavity depths of 3.1mm, 2.6mm and 2.1mm (Mould II). The data was combined by normalizing the results with respect to insert/cavity thickness, 0.5/2.5 mm/mm, shared by the both set-ups. With decreasing insert thickness the peel strength increases in both cases, after a certain thickness ratio, here above 3, saturation is reached and no improvements were reached using thinner inserts (or deeper cavity). This is thought to derive from larger heat capacity of thicker inserts cooling the melt and limiting the penetration of the melt to insert microcavities.

A design of experiments (DOE) approach was applied to study the effect of moulding parameters. Taguchi design matrix was chosen as it is effective for evaluating several factors in early stage of a study [70]. Based on this data an additional analysis of variance (ANOVA) was conducted. The background of ANOVA methods is covered in detail in the literature [71-74] and its full mathematical background is not treated here. For combinations of Taguchi and ANOVA analysis the reader is guided to recent articles, e.g. [75-79].

A standard L_9 four factor –three level (3^4) matrix was used. The experimental matrix and the chosen factors, their levels and the response to be maximized, the peel strength and its signal to noise ratio (S/N ratio) are shown in Table 4. To maximize the number of parameters (factors) to be evaluated, interactions between the parameters were excluded.

Table 4. The parameters, their levels and measured outcome for them. Cavity depth 2.6 mm, insert thickness 0.5 mm. 8-10 samples were measured for each condition. Modified from Publication II.

Run	Mould temperature, °C	Cooling time, s	Injection speed, mm/s	Cylinder temperature, °C	Peel strength, N/cm	S/N ratio for peel strength
I	50	15	10	240–230–220–180	4.1	14.70
II	50	30	20	250–240–230–190	3.8	14.54
III	50	45	30	260–250–230–200	3.3	14.23
IV	70	15	20	260–250–230–200	6.7	15.77
V	70	30	30	240–230–220–180	4.7	14.99
VI	70	45	10	250–240–230–190	8.7	16.33
VII	90	15	30	250–240–230–190	7.7	16.07
VIII	90	30	10	260–250–230–200	14.5	17.44
IX	90	45	20	240–230–220–180	6.1	15.56

The results were analyzed with Minitab™ software, and the main effect plots for both the means and S/N ratios are shown in Fig. 8. The S/N ratio describes the ratio of a mean to its standard deviation and such figures (tables) are an easy way to compare the significance between variables. Based on these two tools, the most important parameter affecting the peel strength was the mould temperature. Both mould temperature and cylinder temperature increase the means and S/N ratio obtained. Physically this is explained by the decrease in the viscosity of the melt and enhancing the penetration of the melt to the microcavities on the insert surface. High injection speed has opposite effect on the adhesion despite its decreasing effect on viscosity. The effect of cooling time on adhesion is lowest on the parameters studied and based on the S/N ratio the significance of the data on cooling time is low.

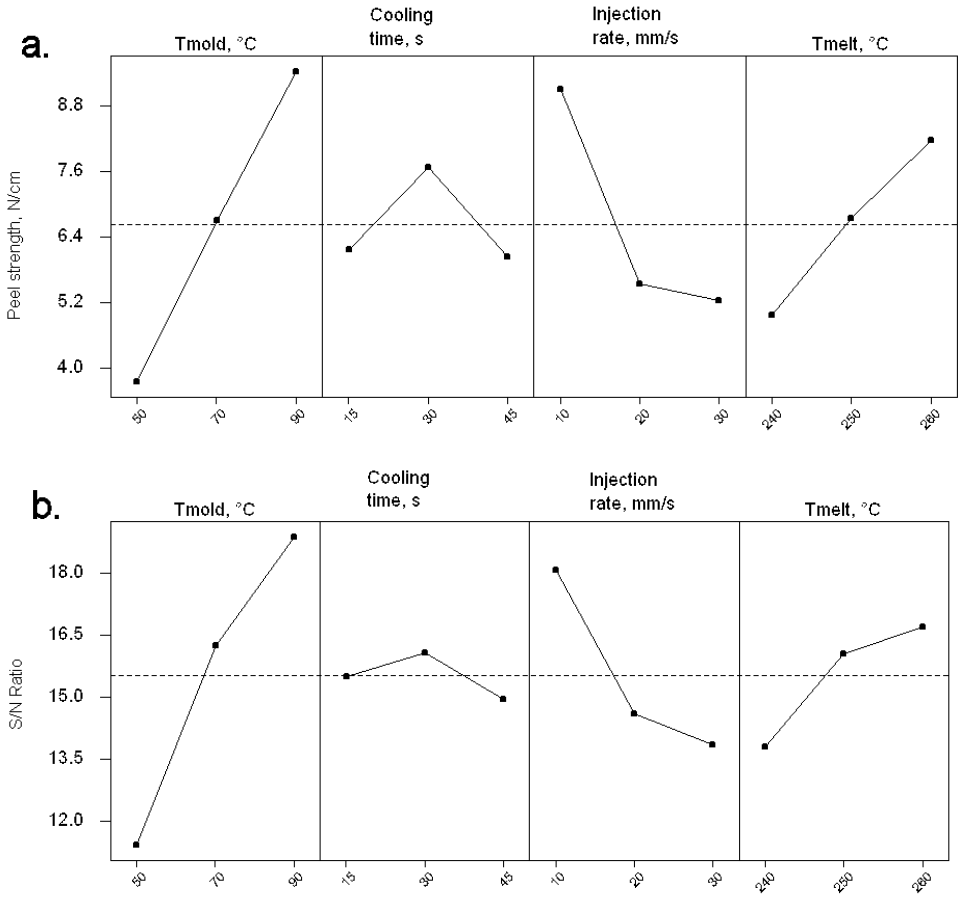

Figure 8. a. Effect of process parameter levels on peel strength. [Publication II, redrawn]
b. Effect of process parameters on S/N ratio (unpublished).

Furthermore, ANOVA was applied to further investigate the significance of the parameters. The mean squared deviation (MSD) of one parameter (explained variation) and total squared deviation (SST, explained + unexplained variation) are needed to obtain the ratio of explained variation to unexplained variation. This yields the variance ratio (F-value), which follow F- distribution and can be used to estimate the significance of the factor on a desired confidence level.

As a saturated design was used, there is no vacant column for the error term. Therefore the error was estimated from the term considered of low significance [71,76], here cooling time (based on the calculated MSD value and S/N curve). The results for the ANOVA analysis are given in Table 5. The limit for 95% confidence is $F_{0.05,\ 2,\ 8} = 4.495$ [73], which means that under these criteria, mould temperature, injection rate and melt temperature are all significant, supporting the data obtained by analysis of S/N ratios.

Table 5. Results on ANOVA analysis on peel strength.

Parameter	Sum of squared deviations	Degrees of freedom	Mean squared deviation (MSD)	F	Percentage contribution, %
Mould temperature	86.38	2	43.19	44.88	64.99
Cooling time (error)	1.92	2	0.96	1	1.45
Injection rate	30.72	2	15.36	15.97	23.11
Melt temperature	13.89	2	6.95	7.21	10.45
Total	132.91	8			100

The work was continued with a confirmation run, using the optimized parameters found to be equal to the run VIII (High mould temperature, moderate cooling time, low injection speed and high cylinder temperatures). When repeating the trial with exactly the same parameter combination, average peel strength of 16.3 N/cm was achieved. This difference in peel strengths between two runs considered identical is mainly arising from the variation of the peel test. As the mould temperature was found out to be the most important parameter, the experiment was repeated using the optimized parameters and higher mold temperature of 100°C resulting even higher average peel strength of 19.7 N/cm.

As discussed in Chapter 2.4, the high insert temperature, possibly in the form of insert pre-heating, has been seen essential for polymer – metal bonding in insert injection moulding. The current results are in line with this, but it is shown that enough heat can be brought to the bondline through monitoring the moulding parameters. Using alternative methods to pre-heating is advantageous due to practical restrictions as well as the possibility of unwanted metal heat treatment. However without insert pre-heating the insert temperature is assumed to be lower than that of the mould due to the extra boundary between the insert and the mould decreasing the total heat transfer. For the same reasons, in all cases, the heat conduction from the melt through the insert is less efficient than through mould wall. So, for detailed information on the interfacial conditions during the injection moulding cycle, mould sensors placed on opposite sides of the cavity could provide valuable information.

Here, low injection velocity was advantageous for bonding. The effect of injection velocity has varied from case to case: in overmoulding of PPS on pre-heated aluminium, the effect of screw velocity was found neglible [23]. Similarly, in the case of butt-joint construction the linear screw velocity was found insignificant, but contributing to strength by parameter interaction [2]. Contrary to this, but supporting the results here, the low injection speed was beneficial for bonding in TPU – γ-AEAPS – aluminium* and TPU – γ-AEAPS – stainless steel hybrids**. Also for these hybrids a higher mould temperature increased the bond strength, but as trade-off between properties, it led to diminishing dimensional accuracy and surface quality of the samples.

In the case of hybrids bonded with chemical coupling agent, a high insert temperature was originally thought to promote the reactions between polymer and coupling agent and also to enhance wetting of the silane layer and possible interdiffusion. Out of the possible factors affecting bonding in polymer – silane interface discussed in Chapter 3.3, the solubilities are dependent on temperature and generally should increase with increasing temperature, as the Gibbs free energy of mixing is reduced. However during the short heat input the silane layer may further cure, reducing the extent of interdiffusion. Also, endothermic chemical reactions are accelerated at higher temperatures, but the activation energy e.g. for urethane reactions with primary or secondary amines is already low at room temperature [80].

Neither the cooling time nor the back pressure affected the bonding in chemically bonded hybrids*. These two parameters were thought to increase the polymer – silane contact and to offer time for the possible chemical reaction or interdiffusion, but neither was observed. However, the delay between surface treatment and moulding is the most influential of the parameters tested and should be kept at minimum. When the silanized inserts are stored for 24 hours, the adhesion is less than half than of the samples moulded within 2–4 hours, assigned to contamination and possible aging of the silane coating **.

6.2 Silane application

As notably high bond strengths were obtained with use of chemical coupling agent, these hybrids were further studied with respect to other main components, i.e. silane layer and metal surface modifications. The moulding parameters were chosen to maximize the bond strength on basis the studies described in Chapter 6.1, with exception of the mould temperature set to 50°C. Without the silane coating there is no measurable adhesion between the TPU and any of the metal substrates.

*Unpublished results
**Originally published in Hoikkanen et al. [81]

To start with silane application conditions, different types of γ-AEAPS solutions were prepared. Application from natural pH 9–10 of γ-AEAPS, from solution acidified with acetic acid to pH 4–4.5 and solution with ethanol/water (9:1) as solvent were compared. The silane coatings, evaluated with sessile drop contact angle and OM, had no differences in the water contact angle and OM showed thin coatings (grain boundaries weakly visible below the coatings); however the coating deposited from ethanol/water based solution had thicker circular patches formed around the irregularities of the surface [**].

The peel strength of TPU – γ-AEAPS – stainless steel hybrids was notably higher for alkaline solution than for acidified solution (Table 6.), agreeing with similar trend reported previously for γ-APS bonded epoxy – AISI 304L stainless steel [39] and later (2011) for γ-APS bonded galvanized steel wires in TPU [82]. The choice of the solvent did not affect the bond strength notably. Comparing to the two studies cited above, in the case of epoxy– γ-APS – AISI 304L, highest strength was obtained with γ-APS deposited from 75:25% ethanol: water based solution, and lowest strength when γ-APS was deposited from 100% ethanol – however, the studied solvent range was limited to 25:75 to 100:0 [39]. In the case of galvanized steel wires, only small improvement in the wire pull-off strength was obtained by changing the of silane solvent from water to ethanol or isopropanol [82].

Table 6. Effect of solvent on peel strength of resulting hybrids. Stainless steel substrates as-received, silane solution concentration 0.5%. [**]

Solvent	Peel strength, N/cm
Alkaline pH, aqueous	87 ± 10
Acidic pH, aqueous	11 ± 7
Ethanol/water, 9:1	78 ± 14

Here, the best conditions, aqueous solutions with natural alkaline pH were used in all other studies. The silane application method was studied next; the methods included were dipping, spraying or brushing. These studies were done with 100 min oxidized stainless steel substrates with 0.5% silane solution and examples of each type of coating as imaged with FESEM are shown in Fig. 9. For comparison the thickest coating obtained by dipping (deposited from 1.0%, with characteristic thick and thin areas) is also shown. The layer thicknesses were measured by scratching the silane layer with a scalpel and studying the fracture surfaces with FESEM from an observation angle of 20–25° [83]. This imaging technique used throughout this work proved to provide valuable information on the silane layer thickness.

[*]Unpublished results
[**]Originally published in Hoikkanen et al. [81]

The sprayed and brushed layers were significantly thicker and smoother than the dipped layers — the layer thickness of sprayed coatings was about 200nm and of brushed ones 500nm. Both the sprayed and brushed coatings were even with a arithmetic averages of profile surface roughness (R_a) of 1 nm, measured with AFM, and no features of the underlying stainless steel topography were visible with FESEM. The scalpel fractured sprayed layer is debonding cohesively so that a thin silane layer stays on the oxide, similarly to dipped coatings. On the contrary, the bulky brushed silane coatings fracture from or close to oxide/coating interface as the structure is similar to bare oxide. When comparing the sprayed and brushed coatings to the thickest silane layer obtained by dipping (1.0%), shown in Fig. 9c, the silane layer seemed to be too thick for the planned application and fractured too easily during the sample preparation, indicative of low strength. To author's knowledge no previous comparisons have been published.

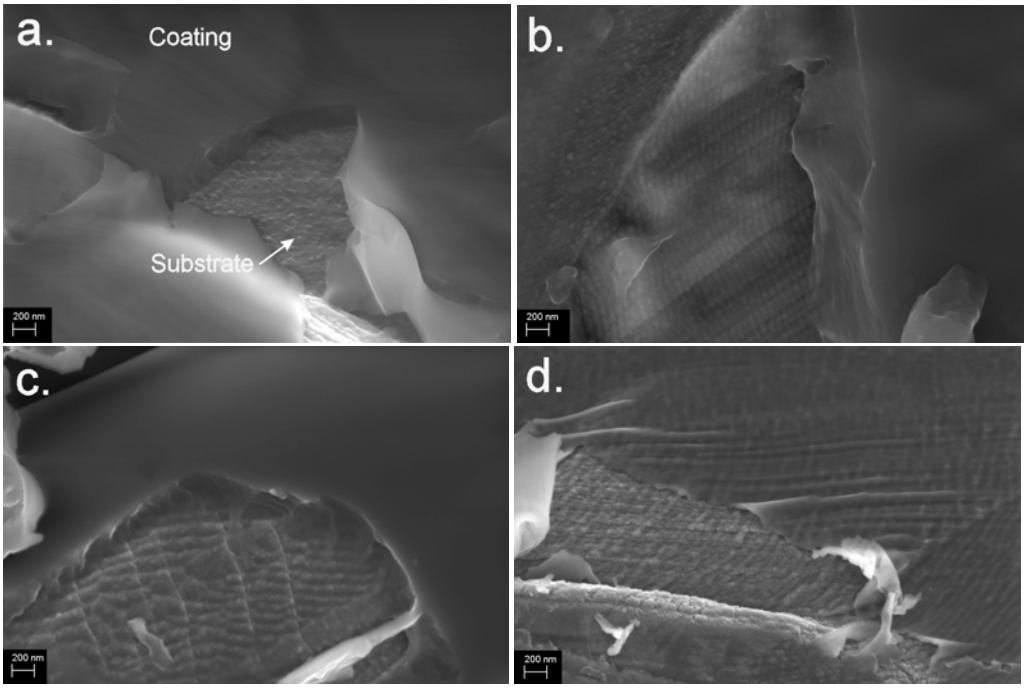

Figure 9. Scalpel fractured **a.** sprayed and **b.** brushed coatings, and **c.** dipped coating (1.0% silane solution), thick middle section and **d.** thin edge section (1.0% silane solution).

The thin silane layers were prepared by deposition from 0.5% silane solution followed by partial desorption of the uncured silane layer in ion-exchanged water (dipping time 1 min) or by deposition from a low concentration silane solution (here 0.1%). The substrate material was stainless steel oxidized at 350°C for 100 min. The desorption method has been applied often [42,46,84], e.g. to increase the evenness of the silane layer, and to produce a thin, covalently bonded layer by removing physisorbed silane [39]. However, the evidence of rinsing benefits are controversial; for example rinsing with alcohol has

been shown to decrease the lap shear strength of epoxy – copper bonds with γ-APS as coupling agent [85], but e.g. in the case of polyurethane – γ-APS – aluminium bonds, rinsing of the silane layer with the deposition solvent increased the fracture energies under all studied deposition conditions [86].

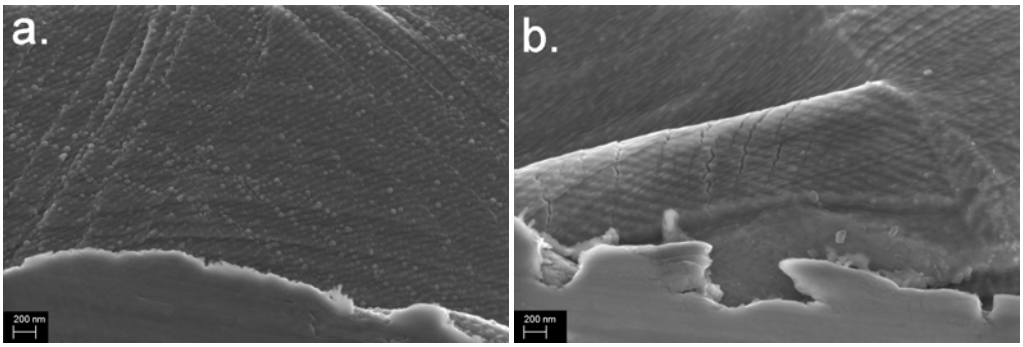

Figure 10. a. Coating from 0.5% silane solution after desorption in water for 1min **b.** Coating from 0.1% silane solution. Substrate 100 min at 350°C oxidized stainless steel.

The thickness (10nm), surface roughness (R_a 7nm) and morphology of the thin silane layers (Fig. 10) produced by desorption were similar to those of silane layers prepared by 0.1% concentration solution having thickness of 10nm and R_a 10nm. As there were no clear visual changes in the thin layers prepared by these two methods, the one with least process steps, i.e. low concentration solution, was chosen for further studies. The peel testing of the hybrids with silane layers deposited from 0.1% solution is discussed in Chapter 6.3.

6.3 TPU – stainless steel hybrids

Silane layer formation

The silane coating formation on stainless steel was studied within the concentration range of 0.1–1.0% on the as-received, electrolytically polished and polished and oxidized substrates with two differing oxidation times. Based on XPS studies, the as-received surface composes of metallic Fe and Cr with a thin surface oxide film of Fe and Cr oxides and hydroxides that are largely covered by carbonous impurities. After electrolytical polishing and 100 min oxidation at 350°C the outer layer is mostly Fe_2O_3. On the other substrates there is no XPS data available but it can be assumed that the islands formed during 5 min oxidation have similar composition as the 100 min oxidized even layer. Based on the literature, the native oxide formed on FeCr alloys after polishing is ~1nm thin and consists of a Cr oxide sub-layer and an outer Fe-rich oxide layer [87,88]. The silane coating thicknesses obtained by studying scalpel fractured silane coatings with FESEM are given in Table 7, together with surface roughness values (R_a) of the coatings and the uncoated substrates.

Table 7. Properties of silane coated stainless steel. For coatings with differences between middle and edge sections of the coating both have been studied.

Surface treatment	Substrate R_a, nm	Silane conc., %	Silane layer R_a (thick/thin section), nm	Silane layer thickness (thick/thin section), nm	Comment
As-received	57	0.1	70	70 / ~0	Rolling lines
		0.25	63	40–100 / ~0	Rolling lines
		0.5	19 / 44	100 / 10	Rolling lines
Electrolytical polishing	1	0.5	18/18	50–230/0–200	Patch formation
Electrolytical polishing + 5 min at 350°C	10	0.1	9	10	
		0.25	3 / 7	50–70 / 10–20	
		0.5	4 / 6	150 / 20	
Electrolytical polishing + 100 min at 350°C	8	0.1	10	10	
		0.25	1 / 6	50–100 / 20	
		0.5	8 / 4	150 / 20	
		1.0	1 / 4	150–300 / 30–80	

For as-received stainless steel, an increase in surface roughness after the coating process indicates patch formation, confirmed by OM and SEM. On as-received substrates coated with a 0.1% solution, silane concentrated on the grain boundaries and other areas were left without coating. With increasing silane concentration the grain boundaries of as-received stainless steel are covered, leading to better coverage. For other substrate types the silane coatings deposited from 0.1% solution were homogeneous and visually uniform with small variations in thickness. The topography of the underlying oxide structure was still clearly observable and thus the thin silane layers had a surface roughness dependent on the roughness of the bare substrate for each substrate type.

Silane coatings from 0.25, 0.5% and 1.0% solutions had structure with two distinctive sections: the middle section of the silane coating on the insert (parallel to the dipping direction) was thick (Fig. 11a) and the rest of the insert had a thin silane coating (Fig. 11b). Inside these sections the coatings were homogenous and uniform. The thickness of the middle section of the coating was assigned to be between 100–300nm depending on the concentration and substrate, and the edge sections were under 20nm for all substrate/concentration combinations. The thick silane coating sections were in general significantly smoother than the uncoated bare substrates as the silane covered the surface irregularities; with the thickest coatings, i.e. coating deposited from 1.0% solution the surface roughness reached 1nm.

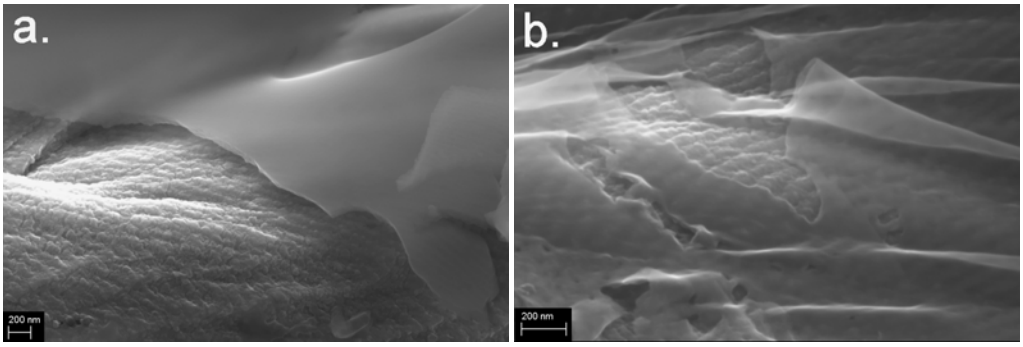

Figure 11. Silane coating deposited from 0.25% silane solution on 100 min oxidized stainless steel substrates. **a.** thick middle section and **b.** thin edge section. [Publication III]

The coating thicknesses for both thin and thick parts of coatings are plotted versus the silane solution concentration in Fig. 12. Polished stainless steel surface has been excluded as there is only one data point available, and also due to patch formation. For controlled oxidized substrates the coating thicknesses are linearly dependent on concentration in the studied range. On the contrary, on as-received stainless steel patches of constant thickness are obtained for the low concentration coatings. Increasing the concentration will lead to formation of even layer and increase in the coating thickness.

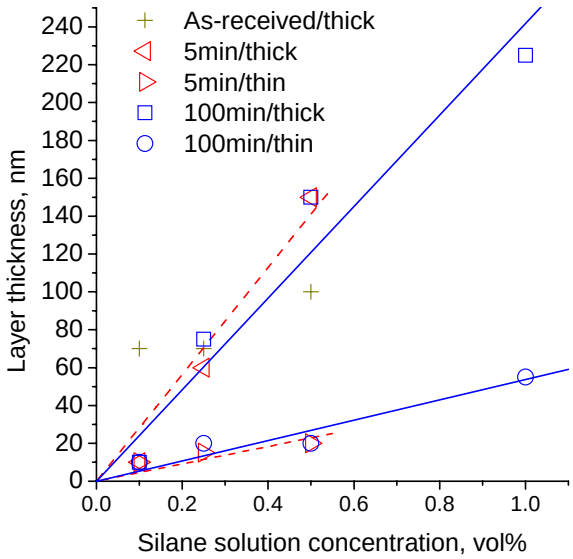

Figure 12. Effect of silane concentration on layer thickness for thin and thick part of the coatings on stainless steel. [Publication III]

Hybrid performance

The adhesion in TPU – silane coated stainless steel was measured by the 180° peel test. The average peel strength from the even peeling region and the fraction of cohesive failure area in TPU are given in Fig. 13. The latter was determined for all samples by image analysis of optical micrographs. Later (Publication VI), the peel strength of polished stainless steel hybrids was measured to be of same range as for oxidized stainless steel. However this data was measured with substantial delay between polishing and silanization and is thus not describing the freshly polished state, but rather long-term ambient oxidation.

The stainless steel surface modification affects the bond strength, but the concentration trend is similar for each substrate type. The oxide microstructure of specimens oxidized at 350°C, islands (5 min) versus thick homogenous oxide layer (100 min), did not affect the bond strength. With low concentrations the bond strength increases rapidly for oxidized substrates but the increase is delayed for as-received substrates. This is thought to derive from the surface roughness, as the minimum thickness of the coating is not increased until the rolling lines have been filled. For each substrate type, the maximum bond strength is reached with a silane solution of 0.5%. A thicker coating was prepared with 100 min oxidized substrate, leading to decline in the bond strength. If assuming that the coating bulk properties are decisive with thicker coatings this can be expanded to all substrates.

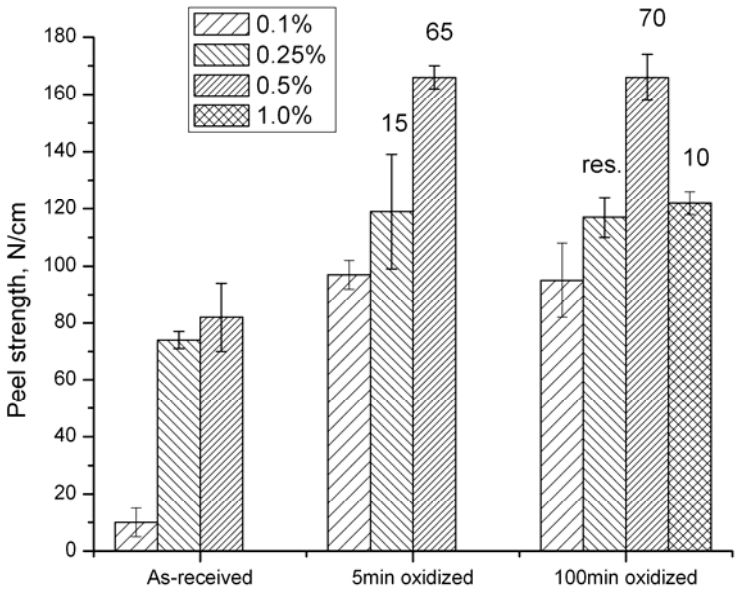

Figure 13. Effect of stainless steel surface treatment and silane concentration on hybrid bond strength and percentage of cohesive failure in TPU (when applicable). Residual (res.) stands for fraction too small to be quantified. 6–10 samples have been used for each condition. [Publication III]

The TPU – stainless steel hybrids with silane coating applied from 0.1% solution with as-received substrates had purely adhesive peel fracture; with both 350°C oxidized substrates the fracture was to a large degree adhesive with traces of TPU on the stainless steel side. The hybrids with 0.25% deposited coatings had adhesive failure for hybrids with as-received substrates and partially cohesive failure for hybrids with oxidized substrates (both oxidization times).

In 0.5% solution silanized samples the peel fracture is adhesive for as-received substrates. The oxidized stainless steel hybrids have mainly cohesive failure in TPU and the failure proceeds in the TPU further from the interface. Besides the cohesive failure in TPU, rest of the fracture is mixed cohesive failure in silane and interfacial TPU/silane failure. In polished stainless steel hybrids (0.5%) the failure was mainly cohesive in TPU and the remained area had strongly interfacial failure between silane and stainless steel oxide. In 1.0% solution deposited on 100 min oxidized sheets the failure proceeds similarly to 0.25% coating on 100 min oxidized sheet. Based on the distribution of the cohesive failure, the thin parts of coating are responsible for load carrying, and this information was used to determine that the optimal silane layer thickness for the studied materials and sample geometry is in the range of a few tens of nanometres.

6.4 TPU – copper hybrids

Silane layer formation

Based on the studies of stainless steel hybrids, two silane solution concentrations were used with copper substrates, 0.25% and 0.50%. The silane layer formation was different for each substrate modification studied: the as-received OFE-OK and Cu-DHP had an uneven layer due to the rolling lines and also on polished OFE-OK and Cu-DHP the silane layer was uneven but to less extent, still showing considerable variation in thickness. On oxidized OFE-OK and Cu-DHP the silane has formed an even, thick layer; however by TEM studies it was shown that the silane layer was thinner on grain boundaries. The silane coating surface roughness and layer thickness are given in Table 8 together with substrate surface roughness values for comparison. With the studied two silane concentrations the thickness of the coating was not affected systematically.

Table 8. Surface roughness and thickness of silane layers on OFE-OK and Cu-DHP, combined data on different specimen used for peel, FT-IR and microscopy.

Surface treatment	Substrate R_a, nm		Silane conc., %	Silane layer R_a, nm		Silane layer thickness, nm		Comment
	OFE-OK	DHP		OFE-OK	DHP	OFE-OK	DHP	
As-received	72	44	0.25	15	9	0–100	0–100	Patch formation
			0.5	18	23	0–100	0–100	Patch formation
Electrolytical polishing	7	13	0.25	21	43	20–100	20–100	Patch formation
			0.5	21	8	20–200	20–200	Patch formation
Electrolytical polishing + 25 min at 200°C	8	11	0.25	22	47	30–35	25	
			0.5	7	70	25–40	25–75	

The chemical composition of the substrates and silane layers was studied with RAIRS. Based on the cuprous oxide (Cu_2O) peak at 650cm^{-1} and the cupric oxide (CuO) peak at 470cm^{-1} [89] the as-received and polished OFE-OK have a mixed Cu_2O / CuO oxide structure, in accordance with previous studies [64,65]. The oxidation treatment at 200°C leads to formation of Cu_2O layer. For Cu-DHP (shown in Fig. 14c) the cuprous oxide band is also evident for oxidized sample (25 min at 200°C) at 650cm^{-1}. For both as-received (Fig. 14a) and polished Cu-DHP (Fig. 14b) there are two or three peaks, one at ~ 665cm^{-1} and two (or one) at 635 and 630 cm^{-1}. These conclusions were supported by TEM data. Also, according to the intensities of the Cu_2O peaks, native Cu oxide layers on the as-received and polished surfaces are much thinner than on the oxidized copper substrates.

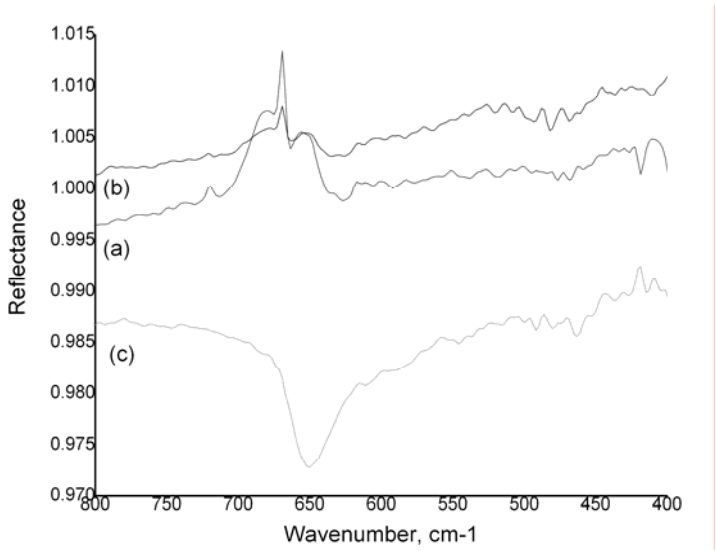

Figure 14. RAIRS spectra of Cu-DHP, region from 800 to 400cm^{-1}. **a.** As-received, **b.** Electrolytically polished and **c.** Oxidized (25 min at 200°C).

The silane coated copper substrates were studied similarly – as an example, the spectra of the silanized Cu-DHP with the silane solution concentration of 0.25% are presented in Fig. 15. In all samples, the intense peaks at 1138 and 1046 cm^{-1} from the crosslinked Si–O–Si stretching vibrations indicated that silane layer has polymerized during the curing at 110°C for 10 min. However, in all samples of Cu-DHP and in the polished OFE-OK with the solution concentration of 0.5%, a weak peak or shoulder at 930 cm^{-1} is observed, indicating a small amount of unpolymerized silanols. In the polished samples, silanized with the solution concentration of 0.25%, the peaks at 1138 and 1046 cm^{-1} are widened and the Si–O–Si band is located at 1110 cm^{-1}, also indicating incomplete polymerization [85,90]. The wide band at around 3300 cm^{-1} corresponding to hydrogen bonded hydroxyl groups was observed in all oxidized samples. The amine peaks at 3420, 3250 and 3160 cm^{-1} are clearly observable in coatings on polished copper while those are weak for coatings on as-received and oxidized samples. It seems that the hydroxyl band at 3300 cm^{-1} is not related to the intensity of Si–OH peak at 930 cm^{-1}, but belongs to absorbed water present in the thick layers.

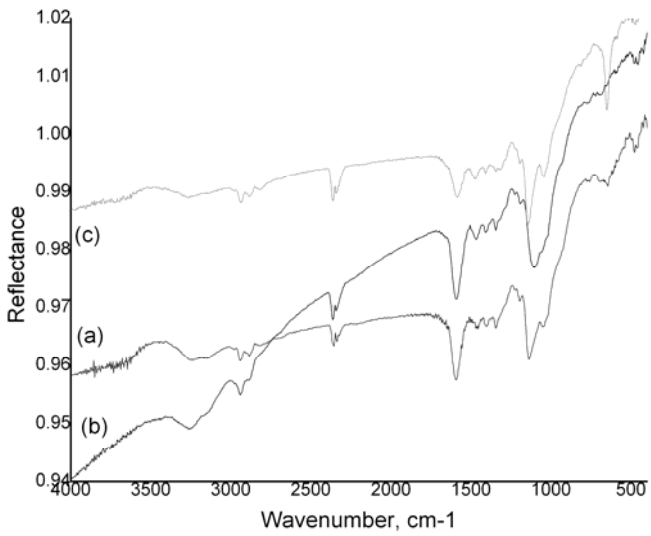

Figure 15. RAIRS spectra of Cu-DHP silanized from 0.25% solution. **a.** As-received, **b.** Electrolytically polished and **c.** Oxidized (25 min at 200°C) substrate.

Hybrid performance

The copper surface modification affected the peel strength and failure type notably (Fig. 16.). Especially the hybrids with thinner silane layers deposited from 0.25% solution had lower strength with as-received or polished substrates than with oxidized substrates.

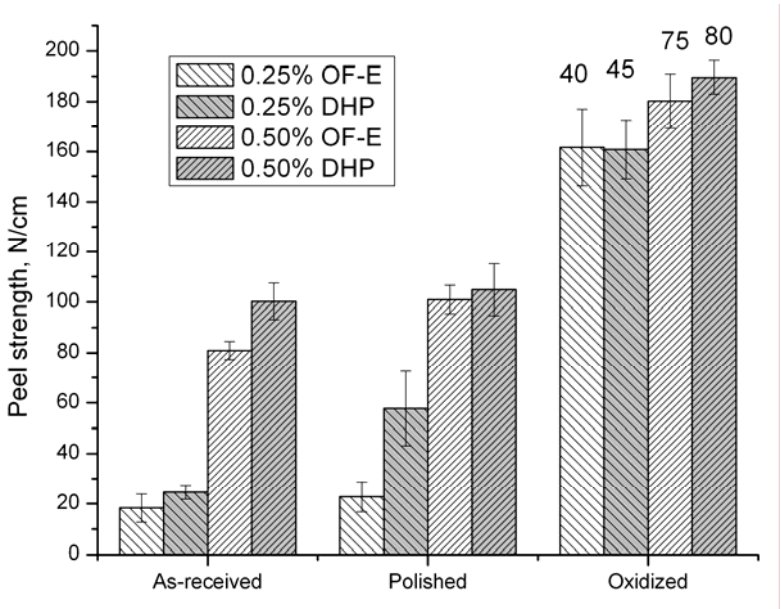

Figure 16. Effect of copper surface treatment and silane concentration on hybrid bond strength and percentage of cohesive failure in TPU (when applicable). 5 samples have been used for each condition.

In the failure surfaces of the as-received copper hybrids no silane was detected with FESEM or AFM due to the rough copper surface. However, with RAIRS, the weak peak related to silane was observed on the copper side indicating failure in the silane layer or adhesive failure between silane and TPU. Probably due to the irregular structure of the silane layer the failure proceeds inside the silane patches. According to FESEM, AFM, and RAIRS studies, the hybrids of polished OFE-OK and Cu-DHP failed inside the silane layer (both concentrations) and also adhesively between silane and TPU (silane deposition from 0.5% solution).

The failure in oxidized OFE-OK and Cu-DHP hybrids was mainly cohesive (75%) in TPU, resulting higher peel strength than measured for the hybrids with other substrate types. The remaining area (25%) had ruptured both adhesively between the silane and TPU and cohesively in the silane layer. With the silane solution concentration of 0.25%, less cohesive failure in TPU (40–45%) was achieved and the other assigned failure types were adhesive failure between silane and TPU, failure in the silane layer, and adhesive failure between oxide and silane. Based on FESEM studies, the grain boundaries were not weakly bonded areas, even if the formation of the silane layer had been disturbed, as the failure did not propagate along grain boundaries.

6.5 TPU – aluminium alloy hybrids

Contrary to other substrate materials, the silane layer on AlMg3 was not observable by FESEM and is deduced to be less than 1–2nm thick. Previously formation of mixed polysiloxane – aluminium oxide layer has been reported due to growth of aluminium oxide during silane deposition [91]. If so, the bulk of the silane layer stays inside the oxide and the layer on the top of the oxide is diminished. Such composite layer leads to an increased modulus of the interfacial layer, compared to the homogeneous, defined layers on copper and stainless steel.

The peel strength for AlMg3 hybrids was 58±18 N/cm (average of 22 samples). The failure path could not be fully identified; based on FT-IR there is residual silane on metal side, but with FESEM silane was not seen on either side of the peeled specimen. However the TPU surface was smooth indicating adhesive failure.

6.6 Environmental durability of hybrids

The environmental resistance of the hybrids was studied with OFE-OK in electrolytically polished condition and oxidized (25 min at 200°C) condition, stainless steel in electrolytically polished condition and oxidized (100 min at 350°C) condition, and NaOH etched AlMg3. These substrates were chosen for their well-defined surface structures with differences in silane layer formation and presumably its bonding to metal surface.

Isohume aging changed neither the visual appearance of the hybrids (Fig. 17a) nor their thermal properties or chemical composition. The glass transition temperature, T_g, of the TPU remained constant, -36°C (2nd heating) and the FT-IR curves were overlapping to those measured from unexposed samples.

After isothermal aging the TPU was slightly yellowed (Fig. 17b), but no changes in the thermal properties were observed. In the FT-IR spectra two new peaks appeared at 2918 and 2850cm^{-1}. These two peaks were also present in the spectra of degraded TPU after 85/85 aging, where also several other changes were observed. Corresponding changes have also been reported after UV irradiation [92], where they were assigned to new methylene groups formed in decomposition. These two peaks also exist in the spectra of silane; and were observed in the interphase region after peeling of freshly prepared samples (Publication III); however it cannot be excluded that these are purely due to degradation of the TPU.

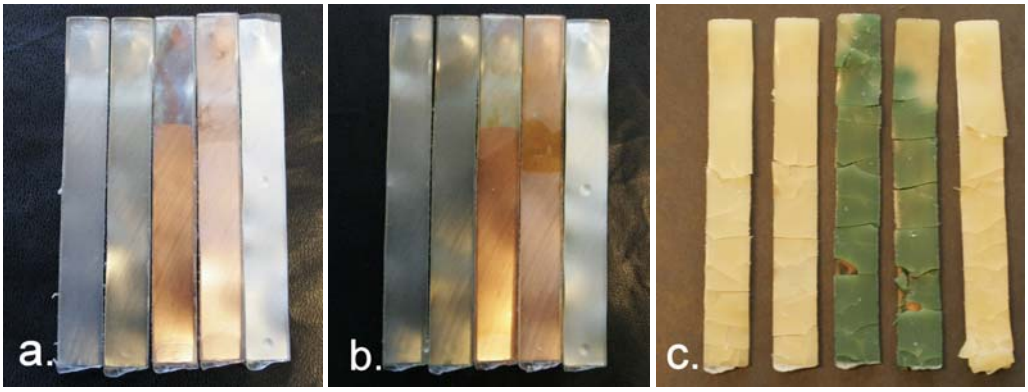

Figure 17. From left: polished stainless steel, oxidized stainless steel, polished OFE-OK, oxidized OFE-OK and AlMg3 hybrids. **a.** After isohume aging. **b.** After isothermal aging. **c.** After hygrothermal aging. [Publication VI]

Hygrothermal aging led to severe degradation of TPU and decohesion of the specimens. TPU of OFE-OK hybrids had drastic change in the colour to green (Fig. 17c), most probably due to Cu ion diffusion into the silane layer [85,93] and further to TPU. Under the combined elevated humidity and temperature, TPU begins to degrade hygrothermally by chain scission [94,95]. The most intense FT-IR peak changed from 1726 to 1698/1692 cm^{-1} i.e from ester carbonyl to urethane carbonyl by degradation of the ester linkage. This is accompanied with changes in the ester C–O stretching region, 1000–1300 cm^{-1} [96]: according to the difference spectra there is reduction at 1216, 1161 and 1061 cm^{-1}. Also thermal behavior was affected; one indication of drop in the molar mass was lowering of T_g to average of -47°C.

The bond strengths measured by peel tests and percentage of cohesive failure in TPU are presented in Fig. 18. As the hygrothermal aging was deterious to the cohesive strength of the TPU, the bond strength could not be determined for these samples.

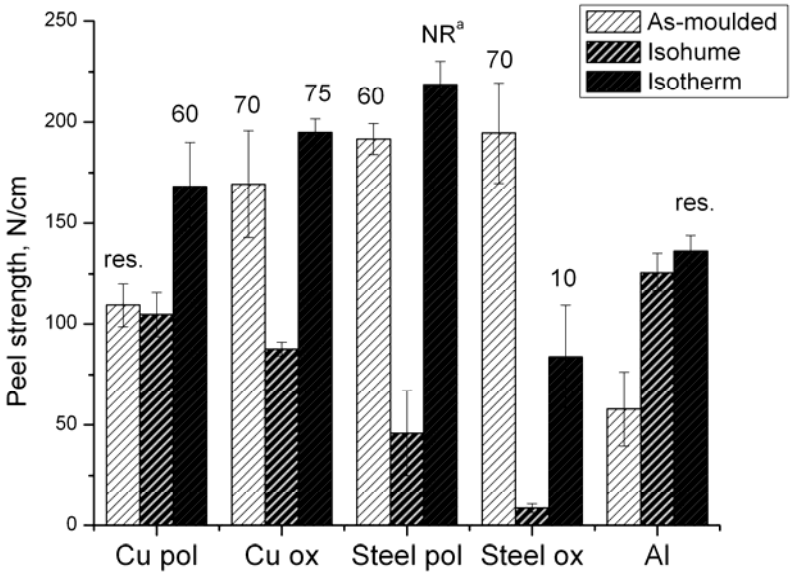

Figure 18. Peel strengths initially and after aging and percentage of cohesive failure in TPU (when applicable). [a]Not representative, all samples ruptured at the beginning of the peel. Modified from Publication VI.

After isohume aging no changes in the TPU were observed, but the bond strength had collapsed, except for AlMg3, and the failure surfaces were purely adhesive for all materials (see collation of failure surface analysis in Table 9. and examples of failure surfaces in Fig. 19.). Phase separation of TPU was observed in peeled polymer sides, but not distinguished with DSC, so it must be limited to the interfacial region. Based on FT-IR, there was remaining silane on all peeled metal surfaces. However, the SEM studies showed that the oxide structure is revealed in oxidized stainless steel hybrids contrary to all other metals which seemed to be covered by silane. The main path for debonding is fracture inside silane layer, caused by depolymerization of the silane network in presence of water, reversible to reaction (2) p. 13.

The isothermal exposure increased the bond strength and the fraction of cohesive failure. The increase in strength is addressed to increased interaction between silane and TPU, as increased number of bonds and extent of diffusion. An exception to this was oxidized stainless steel, which has bond strength lower than initially, and the failure was at least partially interfacial between silane and metal oxide. The silane deposition affecting also the long term behaviour of the hybrids is further discussed in Chapter 6.7.

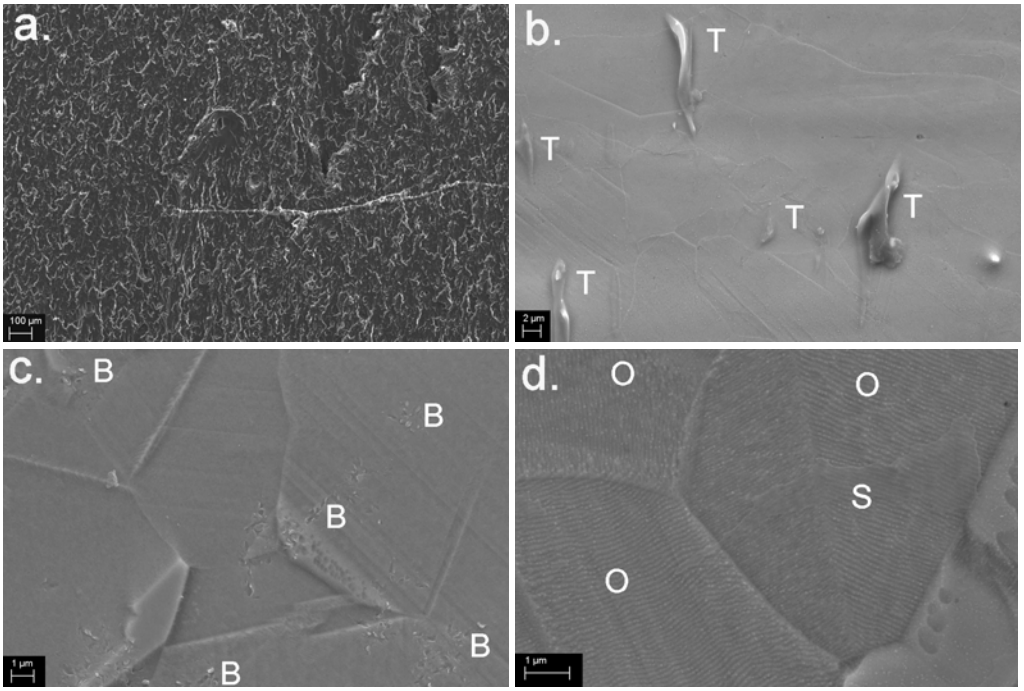

Figure 19. Representative failure surfaces after exposure and peel testing from metal side. Note differing scale bars. **a.** Cohesive failure in TPU (oxidized OFE-OK after isothermal aging). **b.** Few TPU islands (T), silane covering the oxide fine structure (oxidized OFE-OK after isothermal aging). **c.** Broken silane layer (B) (polished stainless steel after isohume aging) **d.** Revealed oxide (O) and a stretch of coating (S) (oxidized stainless steel after isothermal aging).

Table 9. FT-IR and SEM analysis of the non-cohesively fractured peeled hybrids before and after long-term exposure (Publication VI, as-moulded data from Publications III–VI). M and P stand for metal and polymer sides of the fracture surfaces, respectively. Silane solution concentration 0.5%. Modified from Publication VI.

		As-moulded		Isohume		Isothermal	
		FT-IR	SEM	FT-IR	FESEM	FT-IR	FESEM
TPU – Electrolytically polished OFE-OK	M	Silane	Silane	Silane	Probably silane	(Failure in TPU)	TPU and silane islands
	P	-	Silane	-	Phase separation in TPU, no silane detected	-	Silane
TPU – Electrolytically polished +200°C 25 min oxidized OFE-OK	M	TPU	(Failure in TPU)	Silane	Silane/TPU islands	(Failure in TPU)	Few TPU islands
	P	-	-	-	Silane	-	Silane
TPU – Electrolytically polished AISI 304	M	-	(Failure in TPU)	Silane	Silane	(Failure in TPU)	TPU and silane islands
	P	-	-	-	Silane	-	Few silane islands
TPU – Electrolytically polished +350°C 100 min oxidized AISI 304	M	-	(Failure in TPU)	Silane	Silane, oxide	No silane detected	TPU and silane islands
	P	-	-	-	Phase separation in TPU, silane	-	Silane sticks, oxide structure or replica
TPU – AlMg3	M	Silane	No silane detected	Silane	Uncertain	Silane	Uncertain
	P	-	No silane detected	-	Probably silane	-	Probably silane

6.7. Discussion on the concentration and substrate surface state

Different concentrations were studied in Publications III (stainless steel) and V (copper) in combination with several substrate surface modifications. The effect of silane concentration was first studied on stainless steel in a range of 0.1, 0.25, 0.5 and 1.0%, aiming for coating thicknesses from nanometer to micrometer scale. Based on the results obtained, concentrations of 0.25 and 0.50% were used with copper hybrids, and 0.50% with AlMg3 hybrids. With copper the homogeneous coatings on 25 min on 200°C oxidized substrates had a thickness from 25 to 75nm and were unaffected by the concentration in the studied region. In the case of AlMg3 the silane coating thickness was less than 1–2nm. Comparing the cases when a single thickness can be assigned to silane layer, dependence between thermoplastic urethane – metal hybrid bond and the coupling agent layer thickness can be drawn (Fig. 20).

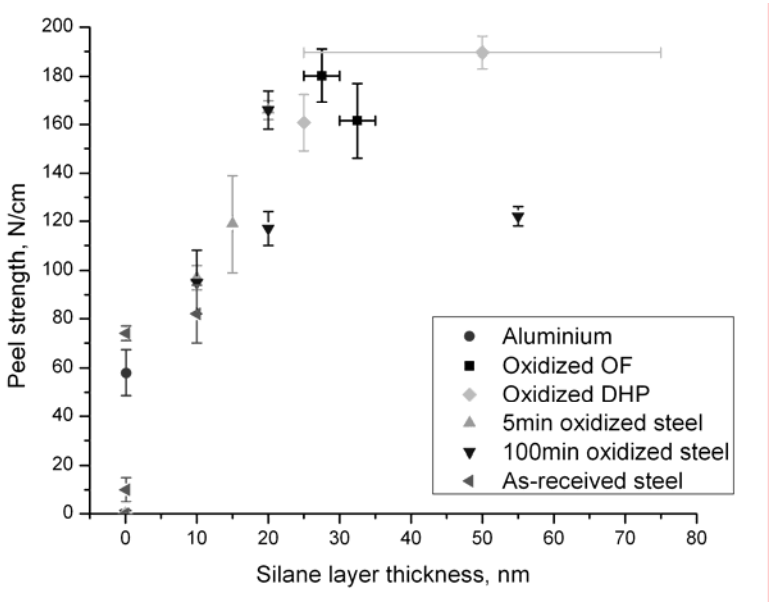

Figure 20. Initial bond strength vs. silane layer thickness. Thickness data based on thin parts of peel samples. Y-error bar shows the double standard deviation. X-error bar shown for OFE-OK and Cu-DHP is the range of measured values.

It has been suggested that a covalently bonded thin silane layer contributes to higher mechanical strength but the optimal layer thickness depends on the system to be bonded [34]. If considering the obtained mechanical strengths with respect to thickness of the coating, up to a certain limit, the thicker the silane coating, the higher the bond strength; after a certain coating thickness the bond strength goes down again. This general trend is thought to be independent of the substrate material, as the failure starts to proceed cohesively inside the bulky silane layer.

The initial strength of polished stainless steel hybrids was superior to as-received state with partially cohesive failure in TPU. Contrary, with polished copper substrates the hybrid strength was either of the same range or marginally better than hybrids with as-received substrates, with no cohesive failure in the TPU. The strengths of oxidized copper, polished stainless steel and oxidized stainless steel hybrids, all with even silane layer, were of the same range, but the initial strength of copper hybrids was more dependent on the surface modification than stainless steel hybrids. This is related to an uneven silane layer with poor bonding to the polished copper surface. Previously similar behaviour has been reported for γ-GPS on degreased copper [53].

The isoelectric points (IEPs) measured for sheet type metals, are 3.0–3.4 for polished AISI 304 stainless steel and 8.7–9.1 for Al with pseudoboehmite layer [97]. For mineral Cu oxides, the IEP values are 5 for synthetic Cu_2O, 11.5 for natural Cu_2O and 7.5–9.9 for CuO of different origins [98]. So, in the silanization conditions used the stainless steel surface is negatively charged and susceptible to form hydrogen bonds with aminosilanes, as seen in low strength after exposure to high humidity conditions. Thus the aminosilane can be partially protonated and bonded to metal oxide up-side down through the aminogroup. However the natural Fe and Cr oxides of polished stainless steel is better bonded than Fe_2O_3 obtained in controlled oxidation — generally the IEP is higher for Cr oxides than for Fe oxides [98].

For copper, it is assumed that the IEP lies between the extreme ends of the given range and thus the extent of the protonation is less than on stainless steel surfaces. The deposition of silane from basic pH solution also causes the cuprous oxide to dissolve in the silane layer (Publication V) (reported also previously [85,93]), increasing the complexity of silane deposition on copper. Probably, the mixed (Cu_2O and CuO) native oxide layers on the as-received and polished copper surfaces are too thin and typically contaminated by carbon [64] to form a uniform and well-bonded silane layer compared to the oxidized copper surfaces with a controlled, uniform silane layer. The silane on AlMg3 is most probably forming an interpenetrating network with the growing oxide and thus at least mechanically bonded to the substrate.

The thickness of the interphase depends on the silane crosslinking conditions [54,55]. Here, the initial precuring temperature was relatively high, leading to a high degree of crosslinks formed and thus only limited interdiffusion and formation of a thick interphase are possible. The bonding conditions either did not offer good possibilities for diffusion, as the melt rapidly cools in the mould, causing a rapid increase in viscosity. However, during the isothermal treatment diffusion is possible. As the silane layer is partially uncrosslinked on the polished copper (Publication V) before moulding it offers best possibility for diffusion. At least a small increase in bond strength after isothermal treatment was observed for all materials except oxidized stainless steel.

The schematic figures (Fig. 21) summarize the differences in the interfacial structures and failure paths between the different hybrids.

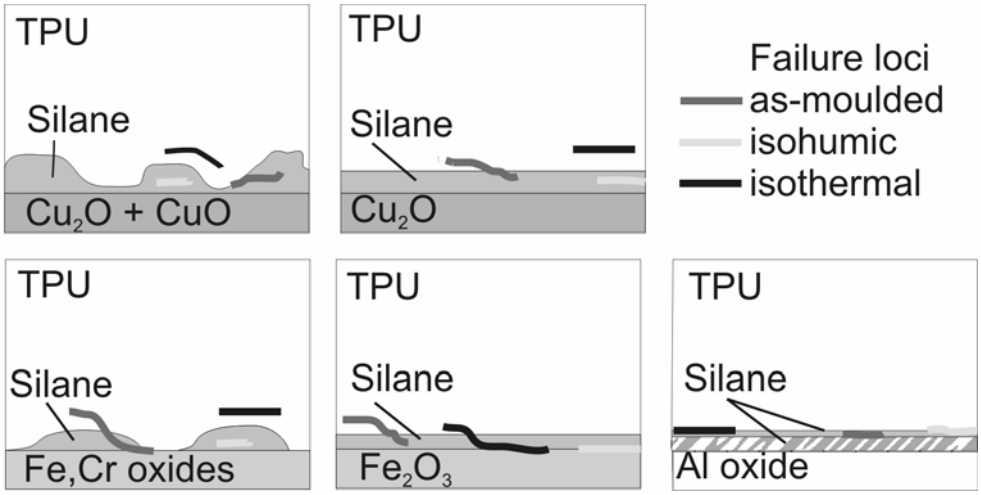

Figure 21. Interfacial regions of the hybrids and failure paths (not in scale). From up left: hybrids of TPU and polished OFE-OK, polished + 200°C 25 min oxidized OFE-OK, polished stainless steel, polished + 350°C 100 min oxidized stainless steel and AlMg3. [Publication VI]

7 CONCLUDING REMARKS

New kind of TPE – metal hybrids were prepared by insert injection moulding. Two approaches were used for adhesion: micromechanical anchoring combined with adhesion modified plastic and use of a chemical coupling agent, here γ-aminoethylaminopropyltrimethoxysilane. With micromechanical anchoring the studies concentrated on the injection moulding parameters. The hybrids bonded with a chemical coupling agent layers were studied with respect to the process parameters in the three main steps: metal surface treatment, role of coupling agent and injection moulding. These were also investigated with hybrids bonded with a chemical coupling agent, but there the focus was set on the effects of substrate material modification and silane application parameters on coupling agent layer formation and TPU – metal hybrid performance.

The micromechanically bonded SEBS – aluminium hybrids were manufactured with two moulds and machines. As there was no information about the mould design to begin with, the effect of polymer/insert thickness ratio was studied first. The results obtained with both moulds were similar and suggest that the thickness ratio is important until approaching a limiting thickness ratio, that was around 3 for the set-up used here. It is assumed that the ratio is dependent on the heat capacities of the insert and polymer melt, as well as the efficiency of heat transfer to the insert and the mould.

When studying the effect of moulding parameters on the adhesion, similar results were obtained both for the hybrids with micromechanical bonding and the use of chemical coupling agent. The most important parameter was the mould temperature: the higher the temperature, the higher the bond strength obtained. Also increased melt temperature and slow injection velocity were beneficial for the adhesion. Though the moulding parameters have been studied for many cases, there is very little generalization done between the individual cases. This is partly due to the nature of injection moulding process, strongly dependent on the part and mould geometry. However it is agreed without exception that raising the insert temperature (within reasonable limits) favours the bonding.

On coupling agent bonded hybrids, γ-AEAPS was found to be an effective coupling agent for bonding thermoplastic urethane to metal by insert injection moulding. The silane application conditions and substrate surface modification influenced the silane layer formation, ultimately affecting the mechanical performace and environmental resistance of TPU – metal hybrids. The best conditions were application from low concentration aqueous alkaline solution by dipping. The substrate surface modification was found to have a clear effect on the silane layer, affecting its evenness and bonding to the metal oxide, as well as its thickness. The effects of silane solution concentration and substrate surface modification were partially complementary. With as-received inserts higher concentration were needed to compensate the surface roughness of the substrate but for even oxide layers the bond strength was less sensitive to silane concentration. FESEM imaging of silane layers was found very useful for quantification of silane layer thickness and its visualization.

Both on as-received stainless steel and copper the silane layer was of varying thickness with silane deposited mainly in the rolling lines. The respective hybrids had failure in the silane layer due to the irregular structure of the silane layer. Also on polished stainless steel and copper the silane formed an irregular structure with silane patches. With thinner silane layers the polished copper surfaces influenced the crosslinking of the silane, as seen by changes in Si–O–Si peaks in FT-IR spectra. With concentrations up from 0.25%, the silane layers on stainless steel had two sections differing in thickness, with a thicker central section and thinner edge sections. The cured silane layer thickness for the oxidized stainless steel substrates was linearly dependent on silane bath concentration. On oxidized copper the silane layer had also positive dependence on the solution concentration within the studied range. However, on the grain boundary areas the silane layer was notably thinner than on the grains.

The highest bond strengths were obtained with oxidized stainless steel and copper substrates. Both with oxidized stainless steel and copper substrates the peel fracture was mainly cohesive in TPU, with a small fraction of mixed cohesive failure in silane and interfacial TPU/silane failure. With stainless steel hybrids, based on comparing the distribution of thickness variation in silane coating to cohesive failure distribution, the cohesive failure in TPU took place in the thin sections and the thick silane layer failed mainly inside the silane layer. Hybrids with as-received substrates failed in the silane layer due to the irregular coating structure and thickness variation in the silane coating. Between the studied copper grades, i.e. high purity, low oxygen content OFE-OK and phosphor alloyed Cu-DHP, there were only small changes in the silane coatings and hybrid performance. The AlMg3 hybrids have bond strength smaller than hybrids of the oxidized stainless steel and copper, due to the high surface roughness of the substrate and the thinness (under 1–2nm) of the effective silane layer.

Common for all studied substrate materials, the coating thickness and the initial hybrid peel strength were positively correlated up to 20–40nm, after which further thickness increase leads to a decrease in mechanical strength. The optimal layer thickness obtained here is low for a massive structure like planar injection moulded hybrid, where thick polymeric coatings have been used [27]. However, in elastomer – metal structures the coupling agent layer needs not to compromise the property divergence of the metal and plastics that lead to generation of residual stresses in case of technical plastics [21], as the low modulus of TPE can compensate for the in-mould and post-mould stresses. Therefore, the transferability of the results to non-elastomeric plastics is questionable.

The environmental resistance of TPU – metal hybrids was studied with several substrates with assumable differences in coupling agent bonding. The studied substrates were polished stainless steel and OFE-OK, polished and 100 min at 350°C oxidized stainless steel, polished and 25 min at 200°C oxidized OFE-OK and NaOH etched AlMg3. Generally, the resistance of hybrids to elevated temperatures is excellent and hybrid performance is limited by the resistance of the TPU matrix, except for TPU – oxidized stainless steel hybrids. Due to hydrolysis of the coupling agent, the bond strength declined after exposure to high humidity for all hybrids studied here, except for TPU–aluminium hybrids. The combination of high humidity and high temperature led to degradation of the polymer (TPU) for all hybrids studied here.

The bond mechanism of the studied hybrids is different for each substrate type. Thus the silane application parameters, e.g. pH and concentration, should be optimized separately for each substrate when applying the approach to new materials. It is possible, e.g. in the case of AlMg3, that silane deposition from higher concentration solution would compensate the surface porosity and thus increase the hybrid bond strength. An option for future research is to aim to improved bond strength and corrosion resistance in wet environments, that has been previously obtained with combinations of silanes and inorganics [99,100]; similar approach could be advantageous here.

The main outcomes of this work are:

1. Insert injection moulded hybrids can be prepared with single step surface preparation of the insert and no specific needs for the injection moulding process. However substrate surface roughness and surface oxide modifications can be used to enhance the bonding.
2. Injection moulding parameters and mould design affect the bond strenth.
3. The surface properties of the substrate material affect the coupling agent layer properties and injection moulded TPU – metal hybrid performance similarly to previously set for thermoset – metal bonds.
4. The conditions for high performance polymer – metal hybrids are: well-known metal surface state, tailored intermediate layer thickness and controlled bonding on both interfaces, injection moulding process set to serve the adhesion and finally, controlled delays between the different steps.

Many questions regarding the processing and properties of injection moulded hybrids still remain open. The scattered data found in the literature lacks general guidelines, for example on the selection of bulk material properties e.g. the process-related shrinkage and differences in material responses to environmental factors. Also, the knowledge on part and mould design is limited, and generality of results obtained is largely unknown. Therefore, it would be beneficial to develop a general test geometry for thermoplastic – metal hybrids, for comparison of results from different research groups. Also specific test methods are needed, as the test set-ups currently used are modified from test methods tailored for other types of structures, like adhesively bonded metal – metal pairs and massive rubber – metal parts. Considerations should also be paid to end of life reusability, or recyclability. Though there remain great challenges, with the increasing interest towards hybrid development, the attractive property profiles of the hybrids may already tomorrow be in practice.

REFERENCES

[1] M. Ashby, *Hybrid materials to expand boundaries of material property space*, J. Am. Ceram. Soc. 94 (2011) S3-S14.

[2] K. Ramani, B. Moriarty, *Thermoplastic bonding to metals via injection molding for macro-composite manufacture*, Polym. Eng. Sci. 38 (1998) 870-877.

[3] F.J. Boerio, P. Shah, *Adhesion of injection molded PVC to steel substrates*, J. Adhes. 81 (2005) 645-675.

[4] G. Zhao, G.W. Ehrenstein, *Investigation of a thin-walled thermoplastic metal hybrid*, SPE ANTEC Tech. Pap. 1999, pp. 1332-1336.

[5] O.J. Zoellner, J.A. Evans, *Plastic-metal hybrid. A new development in the injection molding technology*, SPE ANTEC Tech. Pap. 2002, pp. 2966-2969.

[6] W. Michaeli, R. Maesing, H. Reinartz, *In-mould lamination of metal sheets with integrated forming for metal decorated parts*, SPE ANTEC Tech. Pap. 2010, pp. 735-740.

[7] M.F. Ashby, Y.J.M. Bréchet, *Designing hybrid materials*, Acta Mater. 51 (2003) 5801-5821.

[8] M. Biron, *Thermoplastics and Thermoplastic Composites*. Elsevier 2007. DOI: 10.1016/B978-185617478-7.50010-6.

[9] Y. Estrin, A.V. Dyskin, E. Pasternak, *Topological interlocking as a material design concept*, Mater. Sci. Eng., C. 31 (2011) 1189-1194.

[10] D. Hull, T.W. Clyne, *An Introduction to Composite Materials*, 2nd Ed., Cambridge University Press 1996.

[11] S.-C. Wong, Y.-W. Mai, *Performance Synergism in Polymer-Based Hybrid Materials*. In: S.G. Advani, G.O. Shonaike (Eds.), Advanced Polymeric Materials – Structure Property Relationships. CRC Press 2003, 39p. DOI: 10.1201/9780203492901.ch12.

[12] C.A.J.R. Vermeeren, *An historic overview of the development of fibre metal laminates*, Appl. Compos. Mater. 10 (2003) 189-205.

[13] S. Daykin, *Closing the gap on metals,* Plast. Eng. 64 (2008) 3 28-34.

[14] M. Grujicic, V. Sellappan, L. Mears, X. Xuan, N. Seyr, M. Erdmann, J. Holzleitner, *Selection of the spraying technologies for over-coating of metal-stampings with thermo-plastics for use in direct-adhesion polymer metal hybrid load-bearing components*, J. Mater. Process. Technol. 198 (2008) 300-312.

[15] V. Goodship, J.C. Love, *Multi-Material Injection Moulding*, Rapra Review Reports 13 (2002) Report 145.

[16] M. Grujicic, V. Sellappan, G. Arakere, N. Seyr, M. Erdmann, *Computational feasibility analysis of direct-adhesion polymer-to-metal hybrid technology for load-bearing body-in-white structural components*, J. Mater. Process. Technol. 195 (2008) 282-298.

[17] F. Ehrig, H.-R. Wey, *Foil technology for metal surfaces*, Kunstst. Int. 11 (2007) 72-74.

[18] M. Chen, X. Zhang, Q. Lei, J. Fu, *Finite element analysis of forming of sheet metal blank in manufacturing metal/polymer macro-composite components via injection moulding*, Int. J. Mach. Tools Manuf. 42 (2002) 375-383.

[19] P.F. Bariani, S. Bruschi, A. Ghiotti, G. Lucchetta, *An approach to modelling the forming process of sheet metal-polymer composites*, CIRP Ann. Manuf. Technol. 56 (2007) 261-264.

[20] U. Endemann, S. Glaser, M. Völker, *Strong joint between plastic and metal: assembly technology for plastic-metal hybrid structures*, Kunstst. Int. 92 (2002) 38-40.

[21] W. Zhao, S. Barsun, K. Ramani, T. Johnson, R. King, S. Lin, *Development of PMMA-precoating metal prostheses via injection molding: residual stresses*, J. Biomed. Mater. Res. 58 (2001) 456- 462.

[22] M. Grujicic, V. Sellappan, M.A Omar, N. Seyr, A. Obieglo, M. Erdmann, J. Holzleitner, *An overview of the polymer-to-metal direct adhesion hybrid technologies for load-bearing automotive components*, J. Mater. Process. Technol. 197 (2008) 363-373.

[23] G. Lucchetta, F. Marinello, P.F. Bariani, *Aluminium sheet surface roughness correlation with adhesion in polymer metal hybrid overmolding,* CIRP Ann. Manuf. Technol. 60 (2011) 559-562.

[24] D. Drummer, E. Schmachtenberg, G. Hülder, S. Meister, *MK^2 – a novel assembly injection molding process for the combination of functional metal surfaces with polymer structures,* J. Mater. Process. Technol. 210 (2010) 1852-1857.

[25] J. Nozawa, J. Suda, A.H. Bin Sofian, H. Hagiwara, H. Suda, T. Kawai, T. Komoto, H. Kumehara, *Tribology of polymer injection-molded stainless steel hybrid gear*, Wear 266 (2009) 639-645.

[26] K. Neuking, A. Abu-Zarifa, G. Eggeler, *Surface engineering of shape memory alloy/polymer composites: Improvement of the adhesion between polymers and pseudoelastic shape memory alloy*, Mater. Sci. Eng., A 481-482 (2008) 606-611.

[27] A. Al-Sheyyab, I. Kuehnert, E. Schmachtenberg, *Insert coating as a pre-processing approach for improvement of adhesive bonding in plastic-metal hybrid structures*, SPE ANTEC Tech. Pap. 2007, pp. 1000-1004.

[28] N. Andoh, K. Osumi, *Permanent bond between aluminium and polymer*, Kunstst. Int. 9 (2005) 106-111.

[29] W. Michaeli, A. Neuss, O. Grönlund, C. Lettowsky, *Multi-component technique: Hybrid primary forming of plastics/metal-composites*, Proceedings of 24th Annual Meeting of Polymer Processing Society, Salerno, Italy, June 2008.

[30] P. Walker, *Silane and Other Adhesion Promoters in Adhesive Technology*. In: A. Pizzi, K. Mittal (Eds.), Handbook of Adhesive Technology, 2nd ed., Marcel Dekker, USA 2003, 17p.

[31] M.J. Owen, *Coupling agents: chemical bonding at interfaces*. In: M. Chaudhury, A.V. Pocius (Eds.), Adhesion Science and Engineering, Elsevier 2002, p. 403-431. DOI: 10.1016/B978-044451140-9/50009-3.

[32] K. Weissenbach, H. Mack, *Silane Coupling Agents*. In: M. Xanthos (Ed.), Functional Fillers for Plastics, Wiley VCH Verlag, Germany 2005, p. 59-84.

[33] E.M. Petrie, *Handbook of Adhesives and Sealants*, McGraw-Hill, New York 2007, p. 253-278.

[34] E. Plueddemann, *Silane coupling agents*, Plenum Press, New York 1982.

[35] M.K. Harun, S.B. Lyon, J. Marsh, *A surface analytical study of functionalized mild steel for adhesion promotion of organic coatings*, Prog. Org. Coat. 46 (2003) 21-27.

[36] M.K. Harun, S.N.A.S. Ismail, S.B. Lyon, *Effect of surface pretreatment on water absorption and wet adhesion of organic coatings*, Corros. Eng., Sci. Technol. 41 (2006) 255-258.

[37] M.R. Horner, F.J. Boerio, H.M. Clearfield, *An XPS investigation of the adsorption of aminosilanes onto metal substrates*, J. Adhes. Sci. Technol. 6 (1992) 1-22.

[38] V. Subramarian, W.J. van Ooji, *Effect of the amine functional group on corrosion rate of iron coated with films of organofunctional silanes*, Corrosion 54 (1998) 204-215.

[39] J. Chovelon, L. Aarch, M. Charbonnier, M. Romand, *Silanization of stainless steel surfaces: influence of application parameters*, J. Adhes. 50 (1995) 43-58.

[40] M.K. Harun, J. Marsh, S.B. Lyon, *The effect of surface modification on the cathodic disbondment rate of epoxy and alkyd coatings,* Prog. Org. Coat. 54 (2005) 317-321.

[41] W. Yuan, W. van Ooij, *Characterization of organofunctional silane films on zinc substrates*, J. Colloid Interface Sci. 185 (1997) 197-209.

[42] I. De Graeve, E. Tourwé, M. Biesemans, R. Willem, H. Terryn, *Silane solution stability and film morphology of water-based bis-1,2-(triethoxysilyl)ethane for thin-film deposition on aluminium*, Prog. Org. Coat. 63 (2008) 38-42.

[43] A. Franquet, J. De Laet, T. Schram, H. Terryn, V. Subramanian, W.J. van Ooij, *Determination of the thickness of thin silane films on aluminium surfaces by means of spectroscopic ellipsometry*, Thin Solid Films 384 (2001) 37-45.

[44] D. Zhu, W.J. van Ooij, *Corrosion protection of metals by water-based silane mixtures of bis-[trimethoxysilylpropyl]amine and vinyltriacetoxysilane*, Prog. Org. Coat. 49 (2004) 42-53.

[45] I. De Graeve, J. Vereecken, A. Franquet, T. Van Schaftinghen, H. Terryn, *Silane coating of metal substrates: Complementary use of electrochemical, optical and thermal analysis for the evaluation of film properties*, Prog. Org. Coat. 59 (2007) 224-229.

[46] A.N. Rider, *Factors influencing the durability of epoxy adhesion to silane pretreated aluminium*, Int. J. Adhes. Adhes. 26 (2006) 67-78.

[47] H. Chen, J. Wang, Q. Huo, *Self-assembled monolayer of 3-aminopropyltrimethoxysilane for improved adhesion between aluminium alloy substrate and polyurethane coating*, Thin Solid Films 515 (2007) 7181-7189.

[48] M.A. Petrunin, L.B. Maksaeva, A.I. Marshakov, *The effect of surface siloxane layers on the penetration of hydrogen into iron*, Prot. Met. 37 (2001) 120-125.

[49] J. Flis, M. Kanoza, *Electrochemical and surface analytical study of vinyl-triethoxy silane films on iron after exposure to air*, Electrochim. Acta 51 (2006) 2238-2345.

[50] J. Kim, P. Wong, K. Wong, R. Sodhi, K. Mitchell, *Adsorption of BTSE and γ-GPS organosilanes on different microstructural regions of 7075-T6 aluminium alloy*, Appl. Surf. Sci. 253 (2007) 3133-3143.

[51] D. Susac, X. Sun, K. Mitchell, *Adsorption of BTSE and γ-APS organosilanes on different microstructural regions of 2024-T3 aluminium alloy*, Appl. Surf. Sci. 207 (2003) 40-50.

[52] P. Jussila, H. Ali-Löytty, K. Lahtonen, M. Hirsimäki, M. Valden, *Effect of surface hydroxyl concentration on the bonding and morphology of aminopropylsilane thin films on austenitic stainless steel*, Surf. Interface Anal. 42 (2010) 157-164.

[53] F. Deflorian, S. Rossi, L. Fedrizzi, *Silane-pretreatments on copper and aluminium*, Electrochim. Acta 51 (2006) 6097-6103.

[54] M.K. Chaudhury, T.M. Gentle, E.P. Plueddemann, *Adhesion mechanism of polyvinyl chloride to silane primed metal surfaces*, J. Adhes. Sci. Technol. 1 (1987) 29-38.

[55] A.J. Gellman, B.M. Naasz, R.G. Schmidt, M.K. Chaudbury, T.M. Gentle, *Secondary neutral mass spectrometry studies of germanium-silane coupling agent-polymer interphases*, J. Adhes. Sci. Technol. 4 (1990) 597-601.

[56] W.J. van Ooij, D. Zhu, M. Stacy, A. Seth, T. Mugada, J. Gandhi, P. Puomi, *Corrosion protection properties of organofunctional silanes – an overview,* Tsinghua Science & Technology 10 (2005) 639-664.

[57] D. Zhu, W.J. van Ooij, *Enhanced corrosion resistance of AA 2024-T3 and hot-dip galvanized steel using a mixture of bis-[triethoxysilylpropyl]tetrasulfide and bis-[trimethoxysilylpropyl]amine*, Electrochim. Acta 49 (2004) 1113-1125.

[58] T. Van Schaftinghen, C. Le Pen, H. Terryn, F. Hörzenberger, *Investigation of the barrier properties of silanes on cold rolled steel*, Electrochim. Acta 49 (2004) 2997-3004.

[59] W. Trabelsi, E. Triki, L. Dhouibi, M.G.S. Ferreira, M.L. Zheludkevich, M.F. Montemor, *The use of pre-treatments based on doped silane solutions for improved corrosion resistance of galvanized steel substrates*, Surf. Coat. Technol. 200 (2006) 4240-4250.

[60] M.F. Montemor, A.M. Cabral, M.L. Zheludkevich, M.G.S. Ferreira, *The corrosion resistance of hot dip galvanized steel pretreated with Bis-functional silanes modified with microsilica*, Surf. Coat. Technol. 200 (2006) 2875-2885.

[61] P.H. Suegama, H.G. de Melo, A.A.C. Recco, A.P. Tschiptschin, I.V. Aoki, *Corrosion behavior of carbon steel protected with single and bi-layer of silane films filled with silica nanoparticles*, Surf. Coat. Tech. 202 (2008) 2850-2858.

[62] R.B.C. Cayless, *Alloy and Temper Designation Systems for Aluminum and Aluminum Alloys, Properties and Selection: Nonferrous Alloys and Special-Purpose Materials*, ASM Handbook, Vol 2, ASM International, 1990, pp. 15-28.

[63] K.-T. Wan, A. Di Prima, L. Ye, Y.-W. Mai, *Adhesion of nylon-6 on surface treated aluminium substrates,* J. Mater. Sci. 31 (1996) 2109-2116.

[64] S. Suzuki, Y. Ishikawa, M. Isshiki, Y. Waseda, *Native oxide layers formed on the surface of ultra high-purity iron and copper, investigated by angle resolved XPS*, Mater. Trans. 38 (1997) 1004-1009.

[65] J.-W. Lim, J. Iijima, Y. Zhu, J.H. Yoo, G.-S. Choi, K. Mimura, M. Isshiki, *Nanoscale investigation of long-term native oxidation of Cu films*, Thin Solid Films 516 (2008) 4040-4046.

[66] M. Honkanen, M. Vippola, T. Lepistö, *Oxidation of copper alloys studied by analytical transmission electron microscopy cross-sectional specimens*, J. Mater. Res. 23 (2008) 1350-1357.

[67] M. Honkanen, M. Vippola, T. Lepistö, *Characterization of stainless steel surfaces – modified in air at 350°C*, Surf. Eng. 27 (2011) 325-331.

[68] G. Holden, H.R. Kricheldorf, R.P. Quirk, Thermoplastic Elastomers, 3rd ed., Carl Hanser Verlag, Munich 2004.

[69] Lubrizol General Brochure EMEAI-1. Available from: http://www.lubrizol.com/Engineered-Polymers/Brochure/General-Brochure-EMEAI.pdf, accessed 12.4.2011.

[70] J.P. Lahey, R.G. Launsby, Experimental Design for Injection Molding, Launsby Consulting, USA 1998.

[71] R.J. Del Vecchio, *Understanding design of experiments: a primer for technologists,* Hanser Publishers, Munich 1997.

[72] T.P. Ryan, *Statistical methods for quality improvement*, John Wiley & Sons, New York 1989.

[73] *NIST/SEMATECH e-Handbook of Statistical Methods*, http://www.itl.nist.gov/div898/handbook/, 13.02.2012.

[74] G. Taguchi, *System of experimental design, Vols 1-2*, UNIPUB/Kraus International Publications, White Plains 1987.

[75] R. Ramakrishnan, L. Karunamoorthy, *Modeling and multi-response optimization of Inconel 718 on machining of CNC WEDM process,* J. Mat. Proc. Tech. 207 (2008) 343-349.

[76] W.H. Yang, Y.S. Tang, *Design optimization of cutting parameters for turning operations based on Taguchi method, ,* J. Mat. Proc. Tech. 84 (1998) 122-129.

[77] J.A Ghani, I.A. Choudhury, H.H. Hassan, *Application of Taguchi method in the optimization of end milling parameters,* J. Mat. Proc. Tech. 145 (2004) 84-92.

[78] I. Asiltürk, H. Akkuş, *Determining the effect of cutting parameters on surface roughness in hard turning using the Taguchi method,* Measurement 44 (2011) 1697-1704.

[79] Y. Sahin, *Comparison of tool life between ceramic and cubic boron nitride (CBN) cutting tools when machining hardened steels,* J. Mat. Proc. Tech. 209 (2009) 3478-3489.

[80] Q.-W. Lu, T.R. Hoye, C.W. Macosko, *Reactivity of common functional groups with urethanes: models for reactive compatibilization of thermoplastic polyurethane blends,* J. Polym. Sci., Part A: Polym. Chem. 40 (2002) 2310-2328.

[81] M. Hoikkanen, M. Honkanen, A. Luukkonen, M. Vippola, J. Vuorinen, T. Lepistö, *Thermoplastic urethane – steel hybrids: relationship between steel surface structure and macroscopic properties,* Proceedings of International Rubber Conference, Kuala Lumpur, Malaysia, October 2008.

[82] B. Golaz, V. Michaud, J.-A.E. Månson, *Adhesion of thermoplastic polyurethane to galvanized steel,* Int. J. Adhes. Adhes. 31 (2011) 805-815.

[83] M. Honkanen, M. Hoikkanen, M. Vippola, J. Vuorinen, T. Lepistö, *Electron Microscopy of Silane Layers in Stainless Steel - TPU Hybrids*, Proceedings of 61st Annual Meeting of Scandinavian Society for Electron Microscopy, Stockholm, Sweden, June 2010.

[84] F. Deflorian, S. Rossi, L. Fedrizzi, M. Fedel, *Integrated electrochemical approach for the investigation of silane pre-treatments for painting copper*, Prog. Org. Coat. 63 (2008) 338-344.

[85] X.H. Gu, G. Xue, B.C. Jiang, *Effect of deposition conditions for γ-aminopropyltriethoxy silane on adhesion between copper and epoxy resins*, Appl. Surf. Sci. 115 (1997) 66-73.

[86] N.G. Cave, A.J. Kinloch, *The effect of the silane deposition conditions on the durability of aluminium joints pretreated using 3-aminopropyltrimethoxysilane*, J. Adhes. 34 (1991) 175-187.

[87] A. Vesel, M. Mozetič, A. Zalar, *Oxidation of AISI 304L stainless steel surface with atomic oxygen,* Appl. Surf. Sci. 200 (2002) 94-103.

[88] G. Hultquist, M. Seo, N. Sato, *Selective oxidation of FeCr alloys in the 295-450K temperature range,* Oxid. Met. 25 (1986) 363-372.

[89] B. Lefez, R. Souchet, K. Kartouni, M. Lenglet, *Infrared reflection study of CuO in thin oxide films*, Thin Solid Films 268 (1995) 45-48.

[90] C. Chiang, J. Koenig, *Fourier transform infrared spectroscopic study of the adsorption of multiple amino silane coupling agents on glass surfaces*, J. Colloid Interface Sci. 83 (1981) 361-370.

[91] J. Bertho, V. Stojalan, M-L. Abel, J.F. Watts, *The effect of silane incorporation on a metal adhesive interface: A study by electron energy loss spectroscopy*, Micron 41 (2010) 130-134.

[92] D. Rosu, L. Rosu, C.N. Cascaval, *IR-change and yellowing of polyurethane as a result of UV irradiation*, Polym. Degrad. Stab. 94 (2009) 591-596.

[93] F.J. Boerio, J.W. Williams, J.M. Burkstrand, *The Structure of Films Formed by γ-Aminopropyltriethoxysilane Adsorbed onto Copper*, J. Colloid Interface Sci. 91 (1983) 485-495.

[94] D.G. Thompson, J.C. Osborn, E.M. Kober, J.R. Schoonover, *Effects of hydrolysis-induced molecular weight changes on the phase separation of a polyester polyurethane*, Polym. Degrad. Stab. 91 (2006) 3360-3370.

[95] M.R. Salazar, J.M. Lightfoot, B.G. Russell, W.A. Rodin, M. Mccarty, D.A. Wrobleski, E.B. Orler, D.A. Spieker, R.A. Assink, R.T. Pack, *Degradation of a poly(ester urethane) elastomer. III. Estane 5703 hydrolysis: experiments and modeling*, J. Polym. Sci., Part A: Polym. Chem. 41 (2003) 1136-1151.

[96] R.M. Silverstein, F.X. Webster, Spectrometric Identification of Organic Compounds, 6th ed., John Wiley & Sons, New York, 1997.

[97] G. Lefèvre, L. Čerović, S. Milonjić, M. Fédoroff, J. Finne, A. Jaubertie, *Determination of isoelectric points of metals and metallic alloys by adhesion of latex particles*, J. Colloid Interface Sci. 337 (2009) 449-455.

[98] M. Kosmulski, *Compilation of PZC and IEP of sparingly soluble metal oxides and hydroxides from literature*, Adv. Colloid Interface Sci. 152 (2009) 14-25.

[99] G. Kong, J. Lu, S. Zhang, C. Che, H. Wu, *A comparative study of molybdate/silane composite films on galvanized steel with different treatment processes*, Surf. Coat. Technol. 205 (2010) 545-550.

[100] M.F. Montemor, M.G.S. Ferreira, *Cerium salt activated nanoparticles as fillers for silane films: Evaluation of the corrosion inhibition performance on galvanized steel substrates*, Electrochim. Acta 52 (2007) 6976-6987.

APPENDICES

Table App1. TPU – γ-AEAPS –aluminium/copper/stainless steel experiments. Roman numerals refer to publications.

Substrate	Surface preparation	Substrate evaluation	Silane conc., %	Silane layer characterization				Metal-TPU hybrids			
				FESEM	IR	AFM	Other	Peel testing & failure surface analysis			Other
								Peel	IR	Microscopy	
OFE-OK	As-received	AFM,TEM,IR (V)	0.25, 0.50	V	V	V	TEM (V)	V	V	SEM (V)	
	Electrolytical polishing	AFM,TEM,IR (V)	0.25	V	V	V	TEM (V)	V	V	SEM (V)	
			0.50	V	V	V	TEM (V)	V	V	SEM (V)	Environmental exposure (VI)
	Electrolytical polishing + 25 min at 200°C	AFM,TEM,IR (V)	0.25	V	V	V	TEM (V)	V	V	SEM (V)	
			0.50	V	V	V	TEM (V)	V	V	SEM (V)	Environmental exposure (VI)
Cu-DHP	As-received	AFM,TEM,IR (V)	0.25, 0.50	V	V	V	TEM (V)	V	V	SEM (V)	
	Electrolytical polishing	AFM,TEM,IR (V)	0.25, 0.50	V	V	V	TEM (V)	V	V	SEM (V)	
	Electrolytical polishing + 25 min at 200°C	AFM,TEM,IR (V)	0.25, 0.50	V	V	V	TEM (V)	V	V	SEM (V)	
AISI 304	As-received	AFM(III, IV)	0.1, 0.25	III		III		III	III	OM(III)	
			0.5	III, IV		III, IV	TEM(IV)	III, IV	III	OM(III), SEM, AFM(IV)	
			pH, solvent				OM**, contact angle**	**			
	Electrolytical polishing	AFM(III)	0.50	VI				VI		SEM (VI)	Environmental exposure (VI)

	Electrolytical polishing+ 5 min at 350°C	AFM(III, IV)	0.1, 0.25	III	III		III	III	OM(III)	
			0.5	III, IV	III, IV	TEM(IV)	III, IV	III	OM(III), SEM, AFM(IV)	
	Electrolytical polishing+ 100 min at 350°C	AFM,XPS (III, IV)	0.1, 0.25	III	III		III	III	OM(III)	
			0.50	III, IV	III, IV	TEM, XPS (IV)	III, IV	III	OM(III), SEM, AFM(IV)	Environmental exposure (VI), moulding*
			Application methods	III	III					
			1.0	III	III		III	III	OM(III)	
AlMg3	Etching 5 min in 5%NaOH	AFM(VI)	0.5	VI	VI		VI	VI	SEM (VI)	Environmental exposure (VI), moulding*

*Unpublished, **Hoikkanen et al., [81]

Tampereen teknillinen yliopisto
PL 527
33101 Tampere

Tampere University of Technology
P.O.B. 527
FI-33101 Tampere, Finland

ISBN 978-952-15-2777-7
ISSN 1459-2045